Title
Skap2 is required for β2 integrin–mediated neutrophil recruitment and functions

Journal
Journal of Experimental Medicine, 214(3)

ISSN
0022-1007

Authors
Boras, Mark
Volmering, Stephanie
Bokemeyer, Arne
et al.

Publication Date
2017-03-06

DOI
10.1084/jem.20160647

Peer reviewed

Skap2 is required for β_2 integrin–mediated neutrophil recruitment and functions

Mark Boras,[1] Stephanie Volmering,[1] Arne Bokemeyer,[1] Jan Rossaint,[1] Helena Block,[1] Bernadette Bardel,[1] Veerle Van Marck,[2] Barbara Heitplatz,[2] Stefanie Kliche,[3] Annegret Reinhold,[3] Clifford Lowell,[4,5] and Alexander Zarbock[1]

[1]Department of Anesthesiology, Intensive Care, and Pain Medicine and [2]Gerhard-Domagk-Institute of Pathology, University Hospital Münster, University of Münster, 48149 Münster, Germany
[3]Institute of Molecular and Clinical Immunology, Otto-von-Guericke University Magdeburg, 39106 Magdeburg, Germany
[4]Department of Laboratory Medicine and [5]The Program in Immunology, University of California, San Francisco, San Francisco, CA 94143

Integrin activation is required for neutrophil functions. Impaired integrin activation on neutrophils is the hallmark of leukocyte adhesion deficiency (LAD) syndrome in humans, characterized by impaired leukocyte recruitment and recurrent infections. The Src kinase–associated phosphoprotein 2 (Skap2) is involved in integrin functions in different leukocyte subtypes. However, the role of Skap2 in β_2 integrin activation and neutrophil recruitment is unknown. In this study, we demonstrate the crucial role of Skap2 in regulating actin polymerization and binding of talin-1 and kindlin-3 to the β_2 integrin cytoplasmic domain, thereby being indispensable for β_2 integrin activation and neutrophil recruitment. The direct interaction of Skap2 with the Wiskott–Aldrich syndrome protein via its SH3 domain is critical for integrin activation and neutrophil recruitment in vivo. Furthermore, Skap2 regulates integrin-mediated outside-in signaling events and neutrophil functions. Thus, Skap2 is essential to activate the β_2 integrins, and loss of Skap2 function is sufficient to cause a LAD-like phenotype in mice.

INTRODUCTION

Integrins are heterodimeric transmembrane receptors consisting of α and β subunits. These receptors are expressed on all cells and provide stable adhesion to the extracellular matrix or to ligands expressed on other cells. By forming complex adhesion sites that act as signaling platforms (outside-in signaling), integrins induce migration, cell polarity, proliferation, and survival. As integrins reside in an inactive state in resting cells, integrin activation is required for integrin–ligand binding (inside-out signaling; Herter and Zarbock, 2013). The adhesiveness of integrins (avidity) is regulated by conformational changes in their extracellular domain (affinity) and their distribution on the cell surface (valency; Carman and Springer, 2003). Integrin activation on leukocytes represents a crucial event in cell recruitment during inflammation (Herter and Zarbock, 2013).

Neutrophil migration from the circulation into inflamed tissues proceeds in a cascade-like fashion. Neutrophils attach to, roll along, firmly adhere to, and then crawl over the vascular endothelium before extravasating into the surrounding tissue (Ley et al., 2007). Neutrophil rolling is mediated by interactions with E- and P-selectin, as well as with intercellular adhesion molecule 1 (ICAM-1) present on inflamed endothelium. Binding of selectins to P-selectin glycoprotein ligand 1 (PSGL-1) on neutrophils induces a signaling pathway leading to unfolding of the integrin LFA-1 to an extended conformation with a closed headpiece. This LFA-1 conformation has an intermediate ligand-binding affinity to facilitate slow neutrophil rolling along the endothelium (Kuwano et al., 2010). During rolling, neutrophils are exposed to chemokines presented on inflamed endothelium that bind to G protein–coupled receptors (GPCRs), which induce opening of the LFA-1 headpiece, converting the integrin to a high-affinity state that allows for firm adhesion (Lefort and Ley, 2012). Recruitment of talin-1 and kindlin-3 to the integrin cytoplasmic tail is required for full integrin activation (Moser et al., 2009b; Lefort et al., 2012; Calderwood et al., 2013). After adhesion, neutrophils crawl on the endothelium to reach optimal vascular emigration sites at endothelial junctions. This process depends on the β_2 integrin macrophage 1 antigen (Mac-1; Phillipson et al., 2006; Herter et al., 2013). High-affinity binding of integrins to their ligands induces intracellular signals to the cytoplasm that promote cytoskeletal rearrangements that allow for clustering of integrins at the membrane, increasing their

Correspondence to Alexander Zarbock: zarbock@uni-muenster.de

Abbreviations used: ADAP, adhesion- and degranulation-promoting adaptor protein; AKI, acute kidney injury; CC, coiled coil; GOT, glutamic oxaloacetic transaminase; GPCR, G protein–coupled receptor; GPT, glutamic pyruvate transaminase; GST, glutathione S-transferase; IRI, ischemia reperfusion injury; IVM, intravital microscopy; LAD, leukocyte adhesion deficiency; NET, neutrophil extracellular trap; PAO, phenylarsine oxide; PH, pleckstrin homology; RIAM, Rap1-GTP–interacting adaptor molecule; Skap, Src kinase–associated phosphoprotein; TRAP, thrombin receptor activator peptide; VCA, verprolin homology, cofilin homology, and acidic; WASp, Wiskott–Aldrich syndrome protein.

The Rockefeller University Press $30.00
J. Exp. Med. 2017 Vol. 214 No. 3 851–874
https://doi.org/10.1084/jem.20160647

The Journal of Experimental Medicine

valency. Together, these high-affinity/valency integrin interactions induce neutrophil functional responses, including migration, degranulation, and radical oxygen species production (Herter and Zarbock, 2013).

The Src kinase–associated phosphoprotein 2 (Skap2) is a cytosolic adaptor protein expressed in a variety of cell types including hematopoietic cells (Asazuma et al., 2000; Togni et al., 2005; Alenghat et al., 2012). Skap2 consists of an N-terminal coiled-coil domain (CC domain), a pleckstrin homology domain (PH domain), an interdomain containing two tyrosine phosphorylation sites, and a C-terminal Src-Homology 3 domain (SH3 domain). Skap2 and its related family member Skap1 (found primarily in T cells) have been implicated in cell adhesion through their association to integrins and cytoplasmic actin (Togni et al., 2005). In macrophages, Skap2 is required for global actin reorganization after integrin engagement during cell migration and interacts with different molecules implicated in integrin signaling events, including the adhesion- and degranulation-promoting adaptor protein (ADAP) and Rap1-GTP–interacting adaptor molecule (RIAM; Asazuma et al., 2000; Königsberger et al., 2010; Alenghat et al., 2012). Skap2 itself is found in an autoinhibited conformation in resting cells (Swanson et al., 2008). During cell activation, phosphatidylinositol [3,4,5]-triphosphate (PIP_3) is produced which binds to the PH domain of Skap2 to unfold it, which along with its tyrosine phosphorylation allows Skap2 to associate with its binding partners. Skap2 is also required for tyrosine phosphorylation of ADAP and Sirpα during integrin-mediated adhesion in macrophages and localizes to podosomes during migration (Alenghat et al., 2012; Tanaka et al., 2016). Loss of Skap2 in mice results in reduced inflammation in experimental autoimmune encephalomyelitis as well as defects in macrophage migration into tumor metastasis, suggesting a physiologically important role for leukocyte recruitment in vivo (Togni et al., 2005; Tanaka et al., 2016). However, there have been no studies of Skap2 function in neutrophils or in neutrophil-mediated disease models.

The current study was designed to determine the role of Skap2 in integrin activation and neutrophil recruitment. Using functional ex vivo and in vivo assays, we find that Skap2 is required for selectin- and chemokine-mediated integrin activation and neutrophil recruitment in vivo. Structure-function analysis demonstrated that Skap2 interacts with Wiskott–Aldrich syndrome protein (WASp) in neutrophils and that this interaction is required for WASp-mediated de novo actin polymerization and, consequently, integrin activation. In addition, we showed that Skap2 is involved in integrin-mediated outside-in signaling leading to activation of neutrophil effector functions. In conclusion, we demonstrated that Skap2 is essential to activate β_2 integrins, and loss of Skap2 function leads to reduced neutrophil recruitment in vivo resulting in dramatically lower levels of inflammatory tissue injury in disease models.

RESULTS

Pivotal role of Skap2 for neutrophil recruitment during sterile inflammation

During sterile inflammation, recruitment of neutrophils into the tissue contributes to organ damage and dysfunction (McDonald and Kubes, 2012). To investigate the role of Skap2 in neutrophil recruitment, we performed spinning disk confocal intravital microscopy (IVM) of the mouse liver after inducting hepatic necrosis. In this model, neutrophils start to adhere 30 min after injury, and neutrophil infiltration reaches its maximum at 4 h (McDonald et al., 2010). The initial numbers of adherent cells as well as the time-dependent accumulation of neutrophils were both significantly reduced in *Skap2*$^{-/-}$ mice compared with WT mice (Fig. 1, A–C; and Videos 1 and 2). Reduced neutrophil recruitment in *Skap2*$^{-/-}$ mice resulted in attenuated liver damage as determined by release of glutamic oxaloacetic transaminase (GOT) and glutamic pyruvate transaminase (GPT; Fig. 1, D and E).

To extend our findings, we investigated neutrophil recruitment into the kidney after inducing acute kidney injury (AKI) by renal ischemia reperfusion injury (IRI). In this model, neutrophil infiltration of kidney tissue occurs as early as 4 h after injury and reaches its maximum at 24 h (Friedewald and Rabb, 2004; Li et al., 2007). *Skap2*$^{-/-}$ mice showed a decreased number of neutrophils in the kidney and preserved renal function 24 h after inducing AKI compared with WT mice (Fig. 1, F and G). In WT animals, neutrophil accumulation and AKI were accompanied by massive pathophysiological changes in the outer medulla, whereas only minor kidney damage was observed in *Skap2*$^{-/-}$ animals (Fig. 1, H and I). Reduced neutrophil recruitment furthermore correlated with increased neutrophil counts in the blood of *Skap2*$^{-/-}$ mice (Fig. 1 J). Collectively, these data indicate that Skap2 is required for neutrophil recruitment into inflamed tissue.

TNF-mediated neutrophil recruitment, E-selectin–mediated slow rolling, and GPCR-dependent adhesion are regulated by Skap2

To examine the role of Skap2 in different steps of neutrophil recruitment, we performed IVM of the mouse cremaster muscle after TNF injection. In this model, neutrophil recruitment is dependent on selectin and GPCR signaling (Smith et al., 2004). *Skap2*$^{-/-}$ neutrophils showed significantly elevated rolling velocities and exhibited profound defects in intravascular firm adhesion and extravasation (Fig. 2, A–D). IVM of differentially labeled WT and *Skap2*$^{-/-}$ neutrophils adoptively transferred into WT recipients confirmed that the observed defect in neutrophil recruitment is specifically mediated by the lack of Skap2 in neutrophils (Fig. 2, E–G). Because of their defect in neutrophil recruitment, *Skap2*$^{-/-}$ mice exhibit significant leukocytosis especially in their neutrophil population (Fig. 2 H). However, myeloid maturation markers and physiological relevant surface adhesion receptors are expressed equally on WT and *Skap2*$^{-/-}$ neutrophils (Fig. 2, I and J).

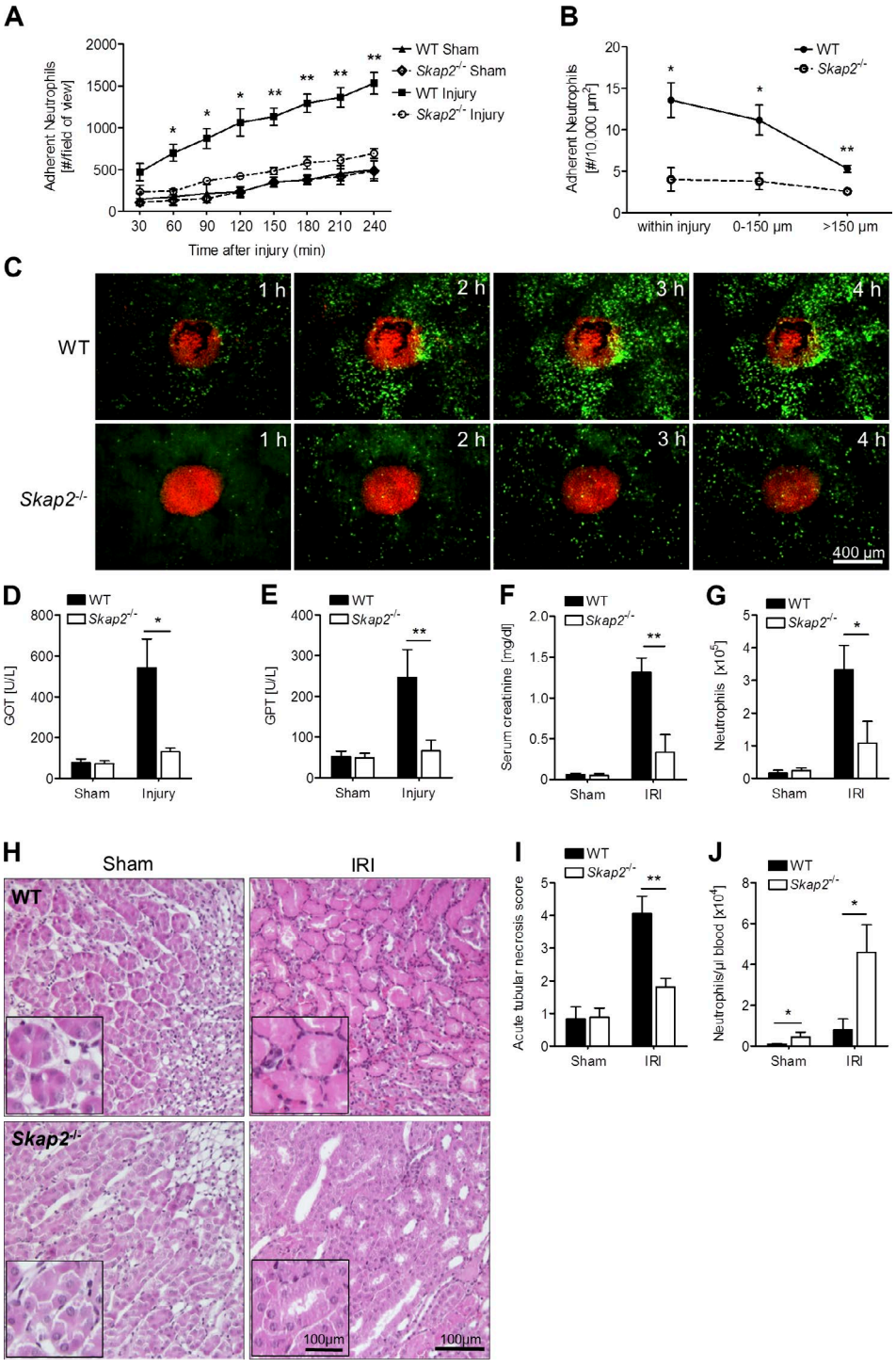

Figure 1. **Pivotal role of Skap2 for neutrophil recruitment during sterile inflammation.** (A–E) Neutrophil recruitment of WT and *Skap2*$^{-/-}$ mice in response to focal hepatic necrosis. (A) Adhesion of neutrophils to the microvascular endothelium after injury or sham operation. $n = 4$ mice/group. (B) Adherent neutrophils within the indicated regions around foci of necrosis 4 h after injury. $n = 4$ mice/group. (C) Representative time-lapse images of neutrophils (green) and area of focal hepatic necrosis (red). (D and E) Serum levels of GOT (D) and GPT (E) 4 h after injury or sham operation. $n = 4$ mice/group. (F–J) Neutrophil recruitment of WT and *Skap2*$^{-/-}$ mice in response to renal IRI. (F) Creatinine serum levels 24 h after IRI or sham operation. $n = 4$ mice/group. (G) Neutrophil numbers per kidney 24 h after IRI or sham operation. $n = 4$ mice/group. (H) Representative hematoxylin and eosin staining of kidney outer medulla 24 h after IRI or sham operation. (I) Acute tubular necrosis scores in kidneys 24 h after IRI or sham operation. $n = 4$ mice/group. (J) Neutrophil counts in blood 24 h after IRI or sham operation. $n = 6$ mice/group. *, $P < 0.01$; **, $P < 0.001$; Student's *t* test. See also Videos 1 and 2. Data are means ± SEM.

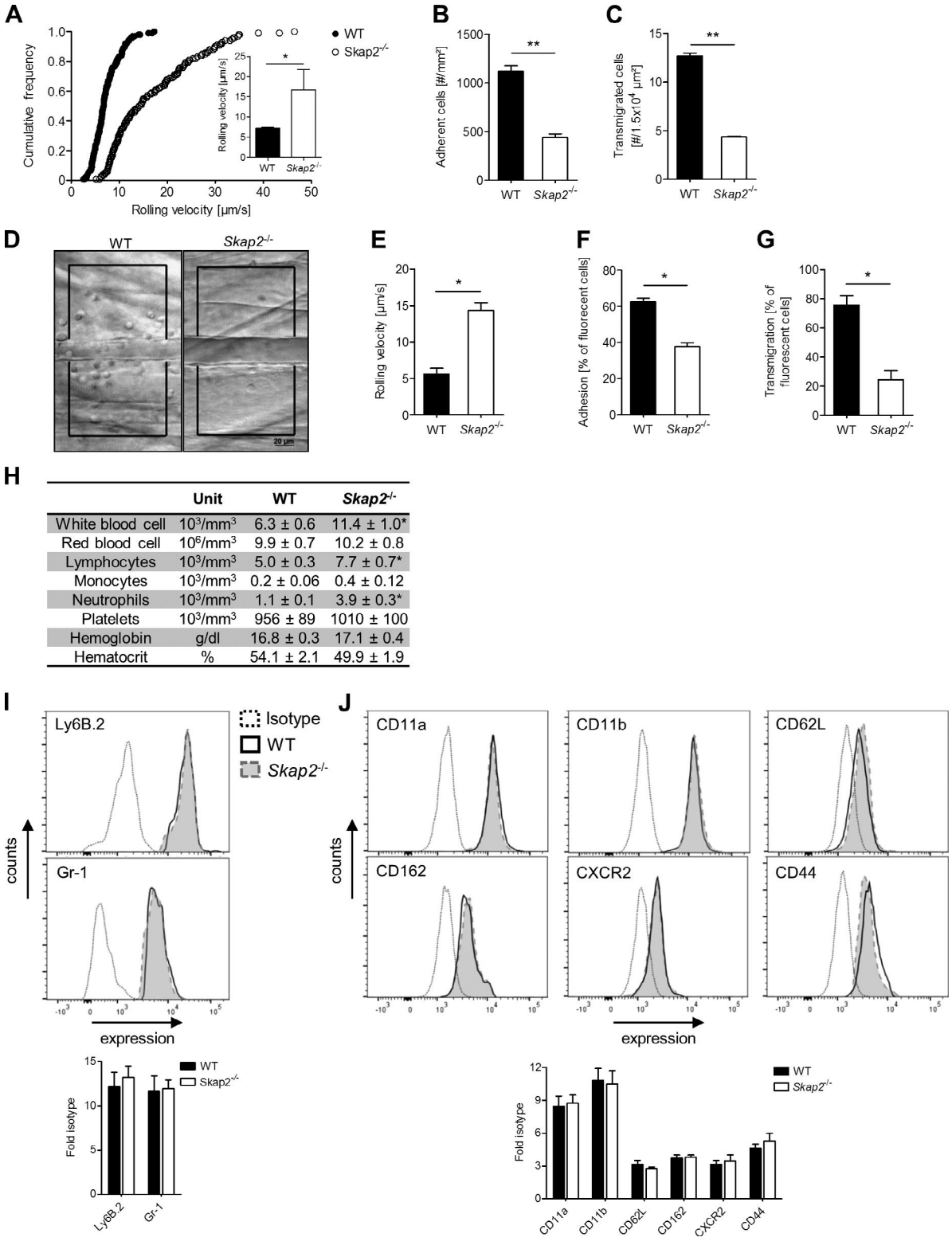

	Unit	WT	*Skap2*$^{-/-}$
White blood cell	$10^3/mm^3$	6.3 ± 0.6	11.4 ± 1.0*
Red blood cell	$10^6/mm^3$	9.9 ± 0.7	10.2 ± 0.8
Lymphocytes	$10^3/mm^3$	5.0 ± 0.3	7.7 ± 0.7*
Monocytes	$10^3/mm^3$	0.2 ± 0.06	0.4 ± 0.12
Neutrophils	$10^3/mm^3$	1.1 ± 0.1	3.9 ± 0.3*
Platelets	$10^3/mm^3$	956 ± 89	1010 ± 100
Hemoglobin	g/dl	16.8 ± 0.3	17.1 ± 0.4
Hematocrit	%	54.1 ± 2.1	49.9 ± 1.9

Figure 2. **Skap2 regulates TNF-mediated neutrophil recruitment.** (A–C) IVM of TNF-inflamed postcapillary venules of WT and *Skap2*$^{-/-}$ mice. (A) Cumulative histogram of rolling velocities. (Inset) Data in a bar graph. 175 data points for each genotype are shown. (B and C) Number of adherent cells (B) and number of extravasated cells (C) 2 h after TNF application. $n = 4$ mice/group. (D) Representative images of transmigrated cells 2 h after TNF application. (E–G) IVM of TNF-inflamed postcapillary venules of WT mice after injection of differentially ex vivo–labeled WT and *Skap2*$^{-/-}$ bone marrow cells. Rolling

Rolling of neutrophils on TNF-inflamed postcapillary venules is mediated by E- and P-selectin. Both selectins have overlapping and redundant functions (Smith et al., 2004; Zarbock et al., 2007). However, because E-selectin is expressed at high densities, it mediates neutrophil slow rolling in vivo (McEver, 2015). When we analyzed E-selectin–mediated slow rolling in vivo and in ex vivo flow chambers, *Skap2*$^{-/-}$ neutrophils showed elevated rolling velocities compared with WT neutrophils (Fig. 3, A and B). Rolling on E-selectin induces the intermediate affinity conformation of LFA-1 as reported by the β_2 integrin antibody KIM127, thereby increasing the affinity for its ligands (Robinson et al., 1992; Kuwano et al., 2010). To take advantage of this tool, we used RNA interference to stably knock down Skap2 in the human HL-60 cell line (Fig. 3 C). Then, control and Skap2 knockdown cells were analyzed in flow chambers coated with E-selectin and the immobilized antibody. Compared with control cells, selectin engagement of Skap2 knockdown cells resulted in significantly reduced numbers of adherent cells on flow chambers coated with KIM127, an antibody that binds selectively to the extended β_2 integrin conformation without affecting their ability to adhere to surfaces coated with TS2/4, an antibody that binds both bent and extended β_2 integrin (Fig. 3 D). This result indicates that Skap2 is directly involved in selectin-mediated integrin affinity regulation.

Next, we investigated the role of Skap2 in GPCR-mediated neutrophil arrest in vivo. In the acutely exteriorized cremaster, neutrophil rolling is mediated by P-selectin, and neutrophil adhesion is almost absent (Ley et al., 1995). Injection of CXCL1 or leukotriene B_4 (LTB_4) induced immediate firm arrest of neutrophils in WT mice. However, neutrophil arrest was significantly reduced in *Skap2*$^{-/-}$ mice (Fig. 3, E and F). Furthermore, *Skap2*$^{-/-}$ mice also showed significantly reduced numbers of adherent and extravasated neutrophils after superfusion of the cremaster muscle with CXCL2 (Fig. 3, G and H). We confirmed the defect in GPCR-mediated adhesion in autoperfused ex vivo flow chambers coated with P-selectin, ICAM-1, and CXCL1 and binding of soluble ICAM-1 after chemokine stimulation (Fig. 3, I and J). Notably, neutrophil adhesion and ICAM-1 binding were intact when *Skap2*$^{-/-}$ neutrophils were stimulated with PMA or manganese (Fig. 3, I and J), indicating that nonchemokine-mediated integrin activation is not affected by the lack of Skap2.

To investigate whether Skap2 is directly involved in GPCR-mediated integrin affinity regulation, we performed flow chamber assays with HL-60 cells on P-selectin, IL-8, and an immobilized antibody directed to the high-affinity conformation of β_2 integrins (mAb24). Knockdown of Skap2 resulted in significantly reduced numbers of adherent cells on flow chambers coated with mAb24 and binding of soluble ICAM-1 after IL-8 stimulation (Fig. 3, K and L), showing that Skap2 is directly involved in chemokine-mediated integrin activation.

Integrin adhesiveness is regulated not only by affinity, but also by valency (clustering; Carman and Springer, 2003). After E-selectin engagement or chemokine stimulation, the vast majority of WT neutrophils exhibited profound LFA-1 clusters, whereas the percentage of *Skap2*$^{-/-}$ neutrophils with clusters was markedly decreased (Fig. 3, M and N).

By analyzing the phosphorylation of known signaling molecules and calcium influx after stimulation with CXCL1, we were able to show that *Skap2*$^{-/-}$ neutrophils have the same phosphorylation of ERK1/2 and p38 and Akt and calcium influx after chemokine stimulation compared with WT neutrophils (Fig. 3, O–R). These data indicate that Skap2 is not involved in the proximal steps of the chemokine signaling cascade.

Skap2 is required for Mac-1–dependent intravascular crawling, extravasation, and chemotaxis of neutrophils

The β_2 integrin Mac-1 has a critical role in the intravascular crawling of leukocytes (Phillipson et al., 2006). To investigate the role of Skap2 in this step, we performed IVM of the cremaster muscle during superfusion with CXCL2. A significantly lower percentage of adherent neutrophils underwent intravascular crawling in *Skap2*$^{-/-}$ compared with WT mice (Fig. 4 A). Furthermore, *Skap2*$^{-/-}$ neutrophils had a reduced crawling velocity and crawled distance (Fig. 4, B–D; and Videos 3 and 4). To verify our in vivo data, we also performed parallel-plate flow chamber assays to analyze crawling of CXCL2-stimulated neutrophils in vitro. Under static and flow conditions, *Skap2*$^{-/-}$ neutrophils showed a significant reduction in crawling velocity and crawled distance compared with WT neutrophils (Fig. 4, E–G). Mac-1 binds various ligands, including fibrinogen (Altieri et al., 1990). When we analyzed the ability of *Skap2*$^{-/-}$ neutrophils to bind soluble fibrinogen, we detected significantly reduced ligand binding after CXCL1 stimulation (Fig. 4 H). To investigate whether the observed defect is caused by abrogated GPCR-mediated affinity regulation of Mac-1, we performed flow chamber assays with Skap2 knockdown HL-60 cells on P-selectin, IL-8, and an immobilized antibody directed to activated Mac-1 (CBRM1/5). Knockdown of Skap2 resulted in significantly fewer adherent cells on flow chambers coated with CBRM1/5 and reduced binding of fibrinogen (Fig. 4, I and J).

Extravasation of neutrophils from the circulation requires efficient chemokine-directed transmigration across the endothelial cell layer (Nathan, 2006). Therefore, we analyzed

velocities (E), number of adherent cells (F), and number of extravasated cells (G) 2 h after TNF application are shown. The percentage of total fluorescent cells for each genotype is shown. $n = 3$ mice/group. (H) Peripheral blood cell counts of WT ($n = 7$) and *Skap2*$^{-/-}$ ($n = 5$) mice. (I and J) Expression of the indicated myeloid maturation markers and cell surface receptors on WT and *Skap2*$^{-/-}$ neutrophils. Black lines show WT, gray dashed lines show *Skap2*$^{-/-}$, and black dotted lines show isotype control. Quantification is shown below. $n = 3$. *, $P < 0.05$; **, $P < 0.01$; Student's *t* test. Data are means ± SEM.

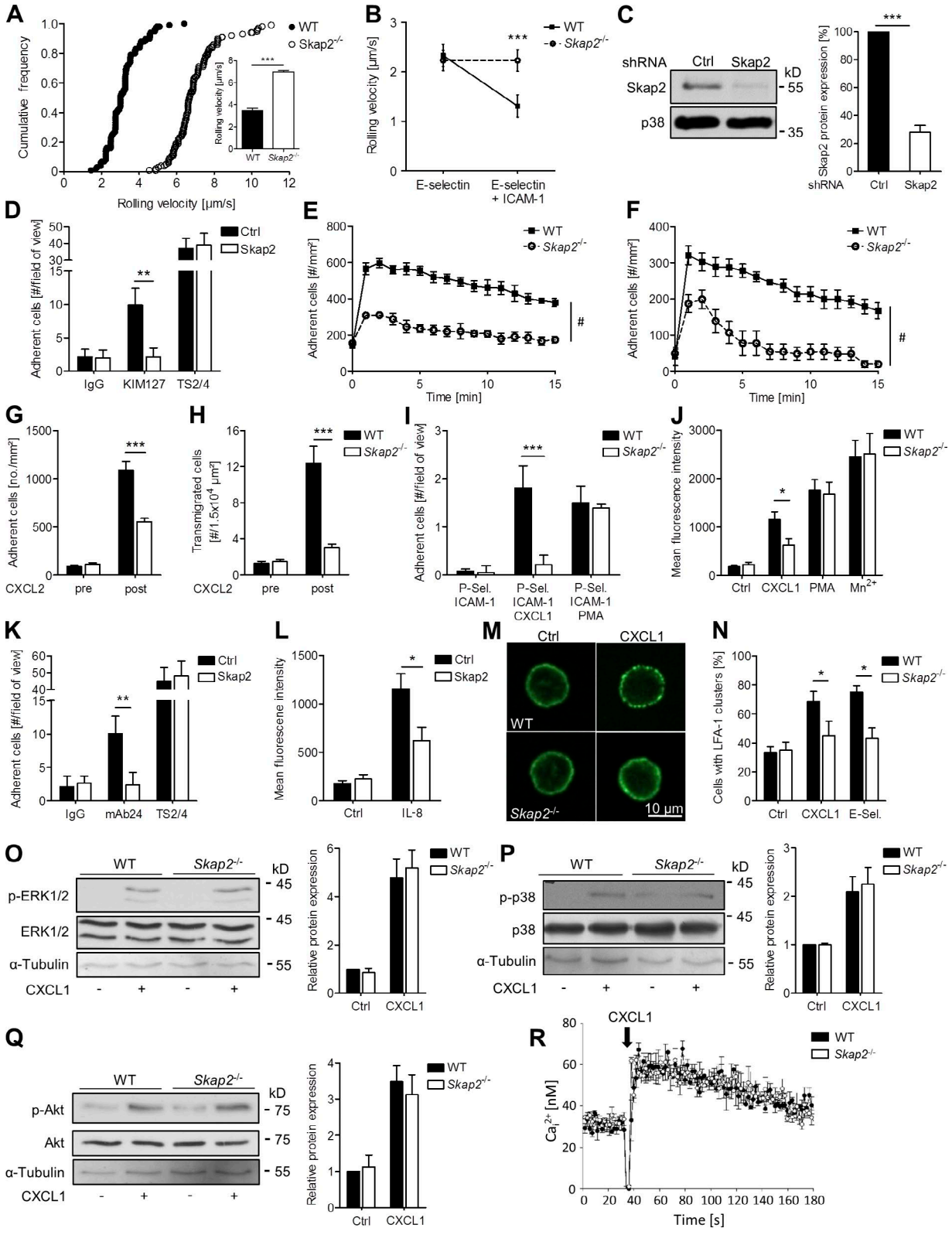

Figure 3. **E-selectin–mediated slow rolling and GPCR-dependent adhesion are regulated by Skap2.** (A and B) E-selectin–mediated slow rolling of WT and *Skap2*$^{-/-}$ neutrophils. (A) In vivo rolling velocities in TNF-inflamed postcapillary venules treated with pertussis toxin and blocking anti–P-selectin antibody. (Inset) Cumulative histogram data in a bar graph are shown. $n = 4$ mice/group. (B) In vitro rolling velocities in autoperfused flow chambers coated

the capacity of *Skap2*$^{-/-}$ neutrophils to transmigrate toward a CXCL1 gradient across endothelial cells in vitro, thereby analyzing transmigration independent of blood circulation. In comparison with WT neutrophils, transmigration of *Skap2*$^{-/-}$ neutrophils was significantly reduced (Fig. 4 K), confirming our in vivo observations.

Considering the defects of *Skap2*$^{-/-}$ neutrophils in the different steps of neutrophil recruitment, we reasoned that Skap2 might affect neutrophil chemotaxis, a complex processes that depends on not only integrin activation, but also on cytoskeletal reorganization and modulation of cell polarization through interconnected signaling pathways (Berzat and Hall, 2010). Therefore, we used time-lapse microscopy to trace neutrophils during chemotaxis in vitro. WT neutrophils readily migrated toward a gradient of soluble CXCL1, but *Skap2*$^{-/-}$ neutrophils showed a profound reduction in migration (Fig. 4 L). Migration velocity, and consequently covered distance, as well as the migration directionality of *Skap2*$^{-/-}$ neutrophils were significantly reduced compared with WT neutrophils (Fig. 4, M–P). Thus, Skap2 is critical for Mac-1 activation, neutrophil crawling, cell motility, and directed chemotaxis.

Crosstalk of Skap2 and WASp is indispensable for β_2 integrin activation and neutrophil recruitment

WASp is involved in β_2 integrin activation and neutrophil functions (Zhang et al., 2006). *Was*$^{-/-}$ and *Skap2*$^{-/-}$*Was*$^{-/-}$ neutrophils showed significantly reduced TNF-mediated neutrophil recruitment (Fig. 5, A–C), CXCL1-mediated firm arrest (Fig. 5 D), and CXCL1-mediated LFA-1 and Mac-1 activation (Fig. 5, E and F). By performing coimmunoprecipitation experiments, we demonstrated that endogenous WASp physically interacts with Skap2 (Fig. 5 G), suggesting that both molecules are involved in the same signaling pathway.

To investigate the interplay of Skap2 and WASp in more detail, we performed pull-down experiments with recombinant domains of Skap2. Recombinant Skap2 and the SH3 domain precipitated endogenous WASp under unstimulated as well as CXCL1- or E-selectin–stimulated conditions, whereas no WASp binding was detectable with the CC or the PH domains (Fig. 5 H). Accordingly, recombinant WASp interacted with recombinant Skap2 or the Skap2 SH3 domain in an in vitro pull-down experiment (Fig. 5 I). In addition, pull-down experiments with the Skap2 SH3 domain bearing the W336K mutation, which impairs its binding to proline-rich proteins and has recently been shown to mediate WASp binding (Macias et al., 2002; Tanaka et al., 2016), revealed this residue to be crucial for Skap2–WASp interaction (Fig. 5 J).

Tyrosine phosphorylation of WASp has been identified as an important physiological regulator of WASp activity (Thrasher and Burns, 2010). However, *Skap2*$^{-/-}$ neutrophils exhibit normal WASp tyrosine phosphorylation after selectin and chemokine stimulation (Fig. 5, K and L), suggesting that Skap2 is not involved in WASp activation. In addition, WASp deficiency does also not alter Skap2 tyrosine phosphorylation after stimulation (Fig. 5, M and N), excluding that WASp is acting upstream of Skap2.

To determine whether co-association of Skap2 and WASp resulted in colocalization of these proteins in neutrophils, we performed a series of immunofluorescence microscopy experiments. Skap2 and WASp were localized in the cytoplasm of unstimulated neutrophils. Chemokine stimulation resulted in translocation of Skap2 and WASp to the plasma membrane where both proteins colocalized (Fig. 6, A and B; Pearson's R; Skap2/WASp unstimulated, 0.38 ± 0.08; and CXCL1, 0.81 ± 0.1; $P < 0.01$). Recruitment of WASp to the plasma membrane was completely absent in *Skap2*$^{-/-}$ neutrophils. To map the domains on Skap2 responsible for recruitment of WASp to the membrane, we used lentiviral transduction of *Skap2*$^{-/-}$ hematopoietic stem cells, followed by transfer of cells into lethally irradiated recipient mice, to reexpress Skap2-mutant proteins in mature neutrophils. Reexpression of Skap2 in *Skap2*$^{-/-}$ neutrophils restored localization of WASp to the membrane after CXCL1 stimulation (Fig. 6, C–E). In contrast, expression of a truncated Skap2 mutant lacking the SH3 domain (Skap2ΔSH3) failed to restore WASp localization to the plasma membrane but did not affect the localization of the Skap2 mutant. In *Skap2*$^{-/-}$ neutrophils reconstituted with a Skap2 R140M mutant, which has been previously shown to impair PIP_3 binding

with E-selectin or E-selectin and ICAM-1. *n* = 4 mice/group. (C) Knockdown of Skap2 in HL-60 cells. Quantification is shown on the right. *n* = 3. (D) Adhesion of control or Skap2 knockdown HL60 cells on flow chambers coated with E-selectin and an isotype, anti-β_2 integrin conformation reporter (KIM127), or anti-β_2 integrin (TS2/4) antibody. *n* = 3. (E and F) Adhesion of neutrophils in postcapillary venules of WT and *Skap2*$^{-/-}$ mice after i.v. injection of CXCL1 (E) or LTB_4 (F). *n* = 4 mice/group. (G and H) IVM of postcapillary venules of WT and *Skap2*$^{-/-}$ mice before or 1 h after superfusion with CXCL2. Number of adherent cells (G) and number of extravasated cells (H) are shown. *n* = 4 mice/group. (I) Adhesion of WT and *Skap2*$^{-/-}$ neutrophils on autoperfused flow chambers coated with P-selectin/ICAM-1 or P-selectin/ICAM-1 and CXCL1 or PMA. *n* = 3 mice/group. (J) Soluble ICAM-1 binding of CXCL1-, PMA-, or Mn^{2+}-stimulated WT and *Skap2*$^{-/-}$ neutrophils. *n* = 3. (K) Adhesion of control or Skap2 knockdown HL60 cells on flow chambers coated with P-selectin, IL-8, and an isotype, anti-β_2 integrin conformation reporter (mAb24), or anti-β_2 integrin (TS2/4) antibody. *n* = 3. (L) Soluble ICAM-1 binding of IL-8–stimulated control or Skap2 knockdown HL-60 cells. *n* = 3. (M and N) LFA-1 clustering on WT and *Skap2*$^{-/-}$ neutrophils. (M) Representative microscopy images. (N) Percentage of cells showing LFA-1 clusters after CXCL1 stimulation in solution or after plating on E-selectin with shear. 50 cells/experiment were analyzed. *n* = 3. (O–Q) WT and *Skap2*$^{-/-}$ neutrophils were stimulated with CXCL1 for 3 min in solution, and lysates were immunoblotted with anti–p-ERK1/2 and anti-ERK1/2 (O), anti–p-p38 and anti-p38 (P), or anti–p-Akt, anti-Akt, and anti–α-tubulin antibody (Q). Quantification is shown on the right. *n* = 3. (R) Concentration of intracellular calcium measured in Indo-1–labeled WT and *Skap2*$^{-/-}$ neutrophils before and after CXCL1 stimulation. *n* = 3. *, $P < 0.05$; **, $P < 0.001$; ***, $P < 0.001$; #, $P < 0.05$ versus all time points; Student's *t* test. Data are means ± SEM. Ctrl, control; E-Sel., E-selectin; P-sel., P-selectin.

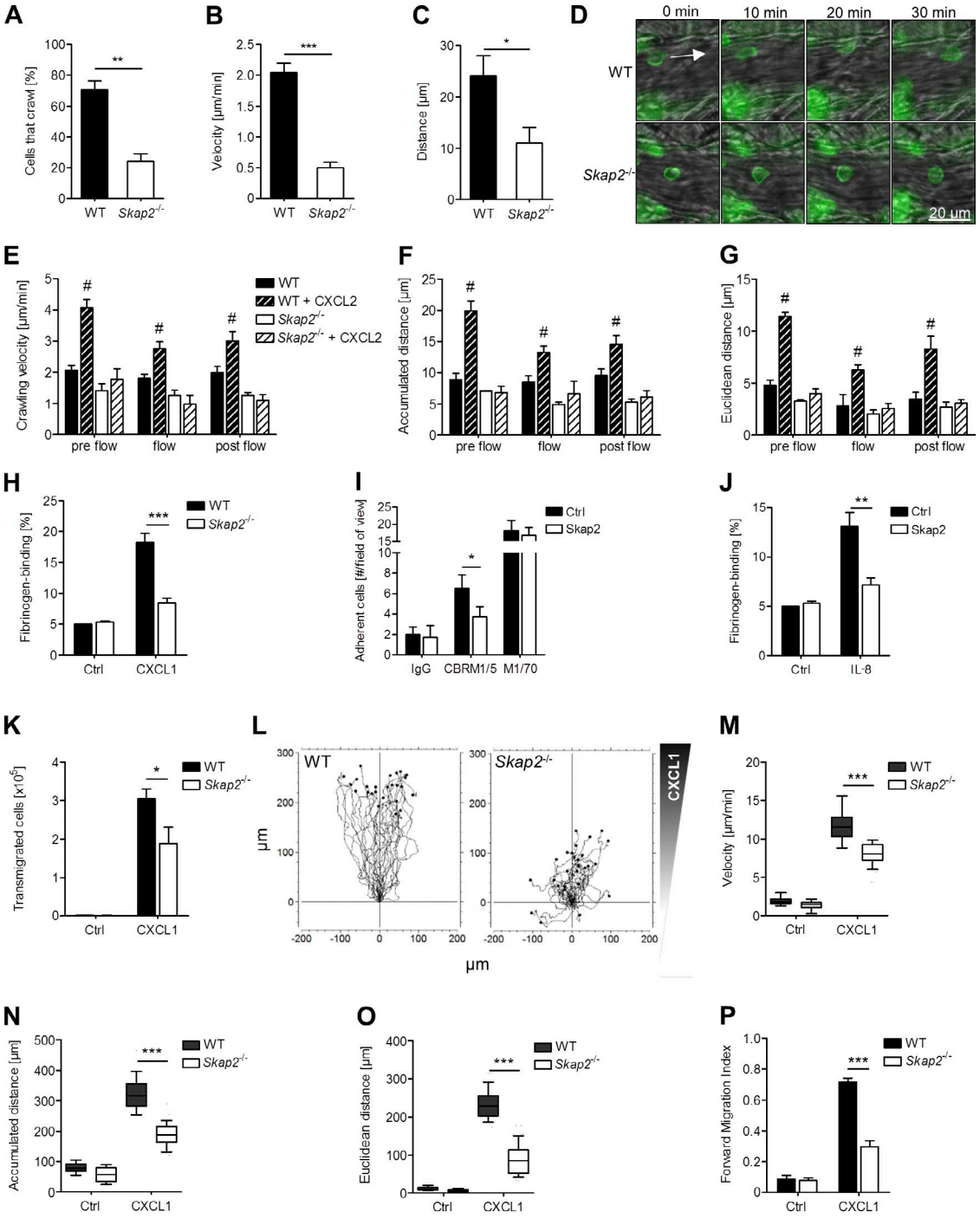

Figure 4. **Skap2 is required for Mac-1–dependent intravascular crawling, extravasation, and chemotaxis of neutrophils.** (A–D) Intravascular crawling of Ly-6G–labeled neutrophils in postcapillary venules of WT and *Skap2*$^{-/-}$ mice during superfusion with CXCL2. (A) Percentage of adherent cells that crawled (A), crawling velocity (B), crawled distance (C), and representative images (D) are shown. The arrow indicates direction of movement. $n = 4$ mice/group. (E–G) Crawling of CXCL2-stimulated WT and *Skap2*$^{-/-}$ neutrophils on serum-coated parallel plate flow chambers in vitro. Crawling velocity (E) and accumulated (F) and Euclidian (G) crawled distance before (preflow), during (flow), and after (postflow) applying flow at 2 dyn/cm^2 are shown. 80 cells/experiment were analyzed. $n = 3$. (H) Soluble fibrinogen binding of CXCL1-stimulated WT and *Skap2*$^{-/-}$ neutrophils. $n = 4$. (I) Adhesion of control or Skap2 knockdown HL60 cells on flow chambers coated with P-selectin, IL-8, and an isotype, anti–Mac-1 activation reporter (CBRM1/5), or anti–Mac-1 (M1/70) antibody. $n = 3$. (J) Soluble fibrinogen binding of IL-8–stimulated control or Skap2 knockdown HL60 cells. $n = 3$. (K) Transmigration of WT and *Skap2*$^{-/-}$ neutrophils through a TNF-stimulated bEnd.5 cell layer in response to a soluble gradient of CXCL1. $n = 3$. (L–P) Chemotaxis of WT and *Skap2*$^{-/-}$ neutrophils in

to the PH domain (Swanson et al., 2008), both Skap2 and WASp failed to translocate to the plasma membrane without affecting PI3K activity (Fig. 6, C–F). To investigate whether the cross talk of Skap2 and WASp is of physiological relevance, we examined the recruitment characteristics of *Skap2*$^{-/-}$ neutrophils expressing WT or mutant versions of Skap2 in TNF-inflamed postcapillary venules. Reconstitution of *Skap2*$^{-/-}$ neutrophils with WT Skap2 restored normal rolling velocity, adhesion, and transendothelial migration, whereas expression of the Skap2ΔSH3 mutant had no effect (Fig. 6, G–I). Expression of WT Skap2 in *Skap2*$^{-/-}$ neutrophils also restored normal CXCL1-induced LFA-1 activation in vitro, whereas expression of the Skap2ΔSH3 mutant did not (Fig. 6 J). However, deletion of the SH3 domain of Skap2 might also disturb binding of other interaction partners. Therefore, we analyzed *Skap2*$^{-/-}$ neutrophils transduced with the Skap2 W336K mutant. Reconstitution with Skap2 W336K also was not able to rescue neutrophil recruitment in TNF-inflamed postcapillary venules or restore CXCL1-induced LFA-1 activation (Fig. 6, K–O). Collectively, these results indicate that interaction of Skap2 and WASp via the Skap2 SH3 domain facilitates translocation of WASp to the plasma membrane during neutrophil activation. The translocation of Skap2 and WASp requires PIP_3 binding by the Skap2 PH domain. Translocation of these proteins to the plasma membrane is required for normal integrin activation and neutrophil recruitment in vivo.

The Skap2/WASp complex triggers actin polymerization, thereby enabling β_2 integrin activation by recruitment of talin-1 and kindlin-3

The actin cytoskeleton is of fundamental role for multiple cellular functions including polarization, adhesion, motility, and redistribution of receptors (Berzat and Hall, 2010). WASp has previously been linked with filamentous actin (F-actin) polymerization and actin dynamics (Zhang et al., 2006; Kumar et al., 2012). Therefore, we analyzed F-actin polymerization in vitro. Stimulation with CXCL1 resulted in significantly reduced levels of F-actin in *Skap2*$^{-/-}$, *Was*$^{-/-}$, and *Skap2*$^{-/-}$*Was*$^{-/-}$ neutrophils or *Skap2*$^{-/-}$ neutrophils retrovirally transduced with the Skap2 W336K mutant (Fig. 7, A and B). By binding of monomeric G-actin, WASp is able to drive formation of branched actin networks through activation of the actin nucleation machinery (Helgeson et al., 2014). To test whether the observed defects in β_2 integrin activation are caused by disturbed actin polymerization in these cells, we used latrunculin A (Lat. A), which binds monomeric G-actin and thereby prevents actin polymerization and assembly. Pretreatment of WT neutrophils with Lat. A significantly suppressed CXCL1-mediated LFA-1 activation and clustering (Fig. 7, C and D), suggesting that actin polymerization is indispensable for the regulation of β_2 integrin affinity and valency. However, pharmacological inhibition of actin polymerization did not further decrease integrin affinity and valency of *Skap2*$^{-/-}$ and *Was*$^{-/-}$ neutrophils (Fig. 7, C and D).

Binding of talin-1 and kindlin-3 to the cytoplasmic tail of β_2 integrins is known to be crucial for integrin activation (Moser et al., 2009b; Shattil et al., 2010). Stimulation of control HL-60 cells resulted in interaction of talin-1 and kindlin-3 with the recombinant β_2 integrin tail (Fig. 7, F and G) as well as endogenous β_2 integrins (Fig. 7, H and I). However, knockdown of Skap2 or WASp as well as inhibition of actin polymerization completely abolished talin-1 and kindlin-3 recruitment to β_2 integrins (Fig. 7, E–I), indicating that actin polymerization is required for recruitment of talin-1 and kindlin-3 to the cytoplasmic tail of β_2 integrins and subsequent β_2 integrin activation. To show specifically that WASp-dependent de novo actin polymerization is crucial for integrin activation, we reconstituted *Was*$^{-/-}$ neutrophils with a WASp mutant lacking the verprolin homology, cofilin homology, and acidic (VCA) domain (WASpΔVCA), which functions as the platform where actin polymerization is initiated (Thrasher and Burns, 2010). Reconstitution with WASp rescues WASp deficiency, whereas the WASpΔVCA mutant failed to restore F-actin polymerization, ICAM-1 binding, and LFA-1 clustering (Fig. 8, A–C).

Binding of talin-1 to the β_2 integrin cytoplasmic tail is a critical final step in integrin activation (Shattil et al., 2010). Inactive talin-1 is cytosolic and in an autoinhibited closed conformation (Moser et al., 2009b). This autoinhibition can be abrogated by the talin activator phosphatidylinositol 4,5-bisphosphate (PIP_2), thereby unmasking the β_2 integrin tail–binding domain (Goksoy et al., 2008; Song et al., 2012). Investigation of inositol phospholipid levels revealed significantly reduced PIP_2 levels after CXCL1 and E-selectin stimulation in *Skap2*$^{-/-}$ and *Was*$^{-/-}$ neutrophils compared with WT neutrophils, without affecting PIP_3 levels (Fig. 8, D and E). Synthesis of PIP_2 from phosphatidylinositol by PI-4 kinase can be inhibited with a low dose of phenylarsine oxide (PAO; Wiedemann et al., 1996; Khvotchev and Südhof, 1998; Várnai and Balla, 1998; Micheva et al., 2001; van Rheenen and Jalink, 2002). Inhibition of PIP_2 synthesis as well as actin polymerization reduced talin-1 plasma membrane localization of WT neutrophils (Fig. 8 F). Furthermore, inhibition of PIP_2 synthesis resulted in reduced association of talin-1 with endogenous β_2 integrins after stimulation (Fig. 8 G). In conclusion, these results show that WASp-mediated de novo actin polymerization and PIP_2 synthesis are required for the association of talin-1 with the β_2 integrin tail.

response to a soluble CXCL1 gradient in vitro. Representative trajectory plots (L), migration velocity (M), accumulated (N) and Euclidean distance (O), and forward migration index of chemotaxing neutrophils (P) are shown. 75 cells/experiment were analyzed. $n = 4$. *, $P < 0.05$; **, $P < 0.01$; ***, $P < 0.001$; #, $P < 0.001$ versus all other groups; Student's *t* test (A–C, H–K, and M–P) or one-way ANOVA (E–G). Data are means ± SEM. Ctrl, control. See also Videos 3 and 4.

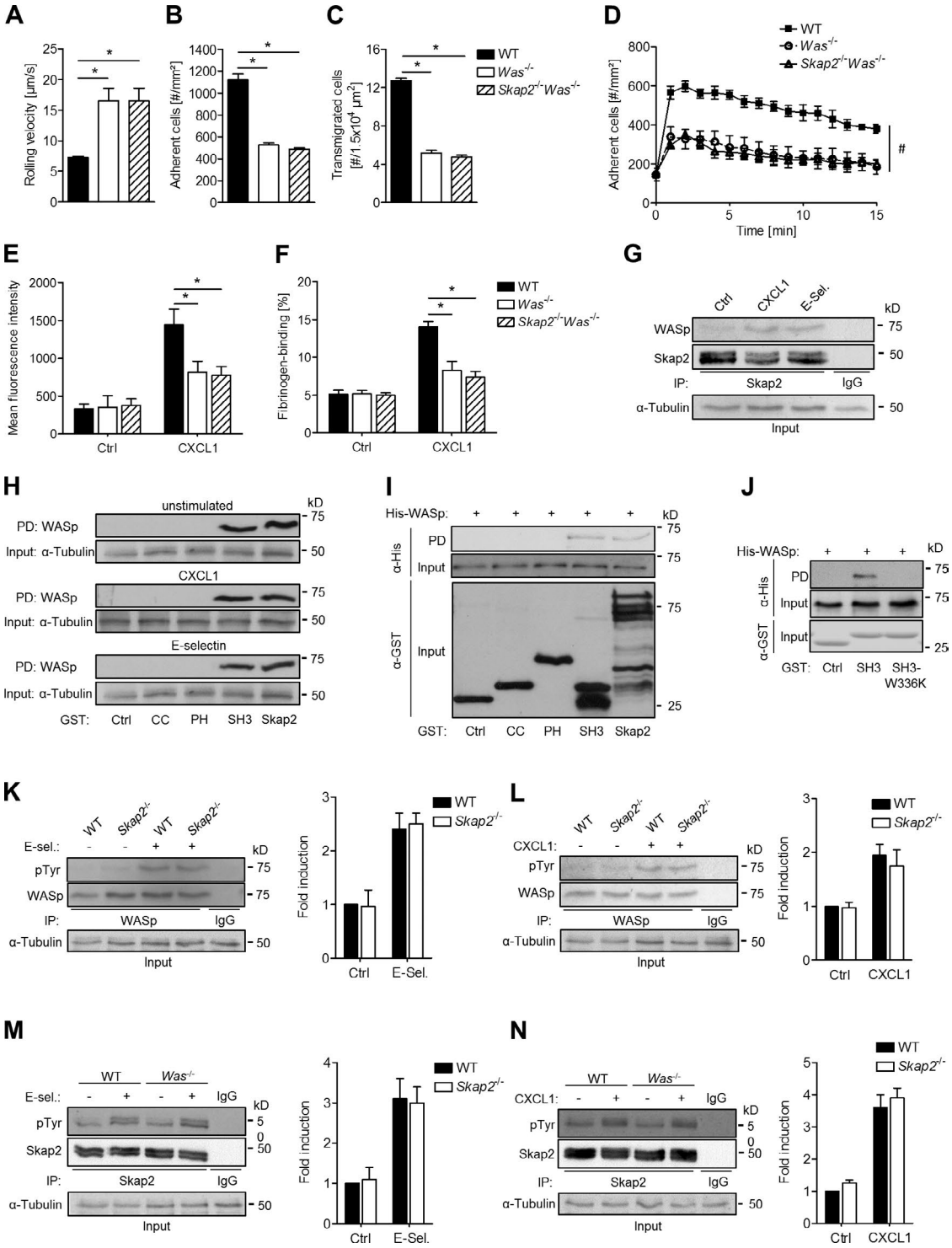

Figure 5. **Cross talk of Skap2 and WASp is indispensable for β_2 integrin activation and neutrophil recruitment.** (A–C) IVM of TNF-inflamed postcapillary venules of WT, *Was*$^{-/-}$, and *Skap2*$^{-/-}$*Was*$^{-/-}$ mice. Rolling velocities (A), number of adherent cells (B), and number of extravasated cells (C) 2 h after TNF application are shown. $n = 4$ mice/group. (D) Adhesion of neutrophils in postcapillary venules of WT, *Was*$^{-/-}$, and *Skap2*$^{-/-}$*Was*$^{-/-}$ mice after i.v. injection of CXCL1. $n = 4$ mice/group. (E and F) Soluble ICAM-1 binding (E) and soluble fibrinogen binding (F) of CXCL1-stimulated WT, *Was*$^{-/-}$, and *Skap2*$^{-/-}$*Was*$^{-/-}$ neutrophils. $n = 3$. (G) Immunoprecipitation of Skap2 in unstimulated WT neutrophils or neutrophils plated on E-selectin with shear or stimulated with CXCL1 in solution. Immunoprecipitates were immunoblotted with anti-WASp and anti-Skap2 antibody. Input was with anti-α-tubulin antibody. $n = 3$. (H) WT neutrophils were left unstimulated, plated on E-selectin with shear, or stimulated with CXCL1 in solution. Lysates were incubated

Skap2 regulates integrin-mediated outside-in signaling

To investigate whether Skap2 is also involved in integrin-mediated outside-in signaling, we analyzed the responses of *Skap2*$^{-/-}$ neutrophils after plating on the multivalent integrin ligand tripeptide Arg-Gly-Asp (pRGD). *Skap2*$^{-/-}$ neutrophils showed a profound defect in integrin-mediated adhesion and spreading (Fig. 9, A–D). Furthermore, integrin-mediated oxidative burst was defective in *Skap2*$^{-/-}$ neutrophils when plated on pRGD or on ICAM-1 and fibrinogen in the presence of TNF (Fig. 9, E–G). However, oxidative burst was unaffected after stimulation with PMA (Fig. 9 H). Integrin-mediated outside-in signaling induces phosphorylation of several signaling molecules. When plated on pRGD, *Skap2*$^{-/-}$ neutrophils exhibit reduced phosphorylation of ERK1/2 and Akt (Fig. 9, I and J), indicating that integrin-mediated outside-in signaling is dependent on Skap2. Additionally, nonadherent *Skap2*$^{-/-}$ neutrophils also showed reduced integrin activation and oxidative burst in response to the co-stimulatory agent TNF, without affecting TNF-mediated up-regulation of the CD11b and CD18 integrin chains (Fig. 10, A–D). Finally, we better characterized neutrophil effector functions of *Skap2*$^{-/-}$ neutrophils and showed that phagocytosis of *Escherichia coli* particles (Fig. 10, E–G) and neutrophil extracellular trap (NET) formation in response to thrombin receptor activator peptide (TRAP)–activated platelets (Fig. 10 H) were significantly reduced in *Skap2*$^{-/-}$ neutrophils. Collectively, these observations provide evidence that Skap2 is additionally involved in other neutrophil functions.

DISCUSSION

Immune responses are highly dependent on tightly regulated integrin activation, thereby ensuring efficient neutrophil recruitment to sites of inflammation (Ley et al., 2007; Phillipson and Kubes, 2011; Herter and Zarbock, 2013). In this study, we identified that Skap2 in neutrophils is required for selectin- and GPCR-induced integrin activation, neutrophil recruitment, and integrin-mediated functions. We demonstrated that Skap2 is indispensable for normal neutrophil slow rolling, arrest, intraluminal crawling, transendothelial migration, and chemotaxis. As a result, *Skap2*$^{-/-}$ mice manifest a leukocyte adhesion deficiency (LAD)–like phenotype. Interaction of Skap2 with WASp via W336 located in the Skap2 SH3 domain facilitates PI3K-dependent translocation of WASp to the plasma membrane and, consequently, neutrophil recruitment in vivo. In addition, we showed that Skap2 specifically regulates integrin affinity and valency by linking Skap2-mediated WASp-dependent de novo actin polymerization to the recruitment of talin-1 and kindlin-3 to the cytoplasmic domain of β_2 integrins. Furthermore, we found that assembly of signaling complexes that trigger integrin-mediated signaling after ligand engagement is also dependent on Skap2, highlighting the crucial role of Skap2 in integrin outside-in signaling leading to activation of neutrophil effector functions. Skap2 also is required for optimal phagocytosis and NET-osis, likely through its role in stimulating actin polymerization via WASp.

The status of integrin activation (intermediate and high-affinity conformation) is dependent on the stimulus (Lefort and Ley, 2012). Chemokines induce high-affinity conformation, whereas selectins force the integrins in intermediate conformation (Lefort and Ley, 2012). Most molecules investigated in the past were involved in either the one or the other pathway. Only very few central molecules including Rap1 and CalDAG-GEFI are required for both pathways (Bergmeier et al., 2007; Stadtmann et al., 2011). Our data provide insights into the intracellular signaling hierarchy between activation receptors and integrin activation. We have demonstrated that Skap2 shares prominent parallels with Rap1, having a general role in integrin activation. Skap2 is involved in β_2 integrin activation and acts like Rap1 as a cell-intrinsic positive regulator for integrin-mediated steps like neutrophil slow rolling, adhesion, and recruitment. One can hypothesize that Skap2 might be required for linking actin polymerization to the binding of kindlin-3 and talin-1 to the cytoplasmic tail of β_2 integrins because we have shown that Skap2 can indirectly regulate actin polymerization via WASp and that, in the absence of Skap2 or WASp or after inhibiting actin polymerization, talin-1 and kindlin-3 are not recruited to the cytoplasmic tail of β_2 integrins. It is also conceivable that the Skap2/WASp complex might additionally assemble important molecules at the plasma membrane that are required for integrin activation because we also found reduced levels of the important signaling intermediate and talin activator PIP_2 in Skap2- and WASp-deficient neutrophils after stimulation. Reduced PIP_2 levels might additionally influence talin-1 recruitment and integrin activation. In line with this finding, inhibition of PIP_2 synthesis by PAO abolished recruitment of talin-1 to β_2 integrins. However, not much is known about the specificity of the inhibitor. It will be of interest to verify these results with specific depletion of PIP_2. Despite the clear evidence emphasizing the role of kindlin-3 in integrin activation and function, the underlying mechanism that is required for the recruitment of kindlin-3 to the β_2 integrin

with GST alone (control), GST fusion proteins of the Skap2 CC, PH, or SH3 domains, or full-length Skap2. Precipitates were immunoblotted with anti-WASp, and input was with anti–α-tubulin antibody. $n = 3$. (I and J) In vitro co-purification of His-WASp by different Skap2 GST fusion proteins. Precipitates were immunoblotted with anti-His or anti-GST, and input controls were with anti-GST antibody. $n = 3$. (K–N) WT and *Skap2*$^{-/-}$ or *Was*$^{-/-}$ neutrophils were left unstimulated, plated on E-selectin with shear, or stimulated with CXCL1 in solution. Lysates were immunoprecipitated with anti-WASp (K and L) or anti-Skap2 (M and N) antibody followed by immunoblotting with anti-phosphotyrosine (4G10), anti-WASp, or anti-Skap2 antibody. Input was immunoblotted with anti–α-tubulin antibody. Quantification is shown on the right. $n = 3$. *, $P < 0.05$; #, $P < 0.05$ versus all time points; Student's *t* test (A–D and K–N) or one-way ANOVA (E and F). Data are means ± SEM. Ctrl, control; E-Sel., E-selectin; IP, immunoprecipitate; PD, precipitate.

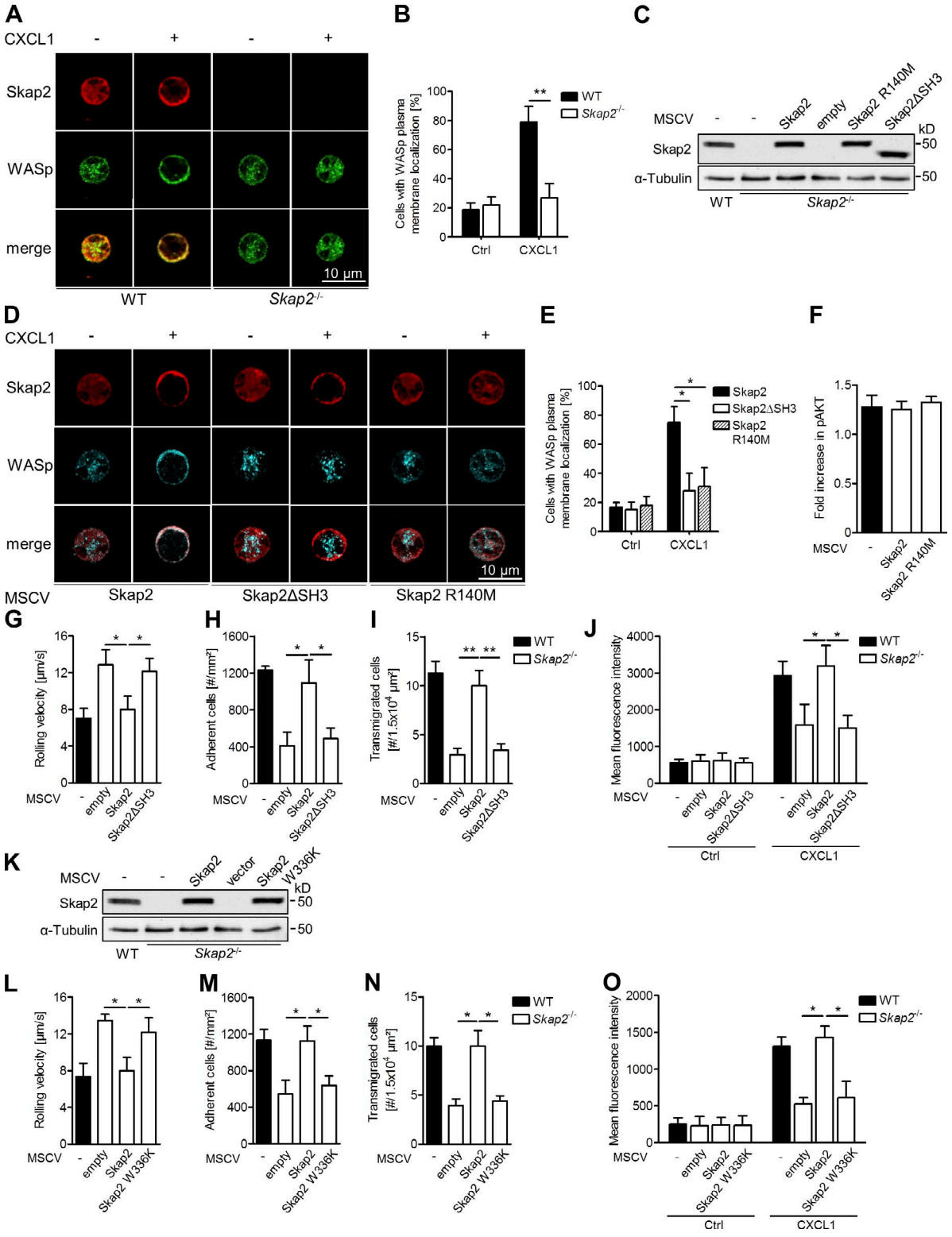

Figure 6. **The Skap2 SH3 domain mediates WASp localization and integrin activation.** (A and B) Subcellular localization of Skap2 and WASp in unstimulated or CXCL1-stimulated WT or *Skap2*$^{-/-}$ neutrophils. (A) Representative microscopy images. (B) Statistics of WASp plasma membrane localization. 75 cells/experiment were analyzed. $n = 3$. (C) Expression of Skap2 in WT, *Skap2*$^{-/-}$, and *Skap2*$^{-/-}$ neutrophils reconstituted with Skap2, vector control, Skap2 R140M, or Skap2ΔSH3. Lysates were immunoblotted with anti-Skap2 and anti–α-tubulin antibody. $n = 2$. (D) Subcellular localization of Skap2 and WASp in unstimulated or CXCL1-stimulated *Skap2*$^{-/-}$ neutrophils reconstituted with Skap2, Skap2ΔSH3, or Skap2 R140M. $n = 3$. (E) Statistics of WASp plasma

tail is still unknown. Elucidating this mechanism will be the focus of future studies. Our data are in line with previous studies suggesting that Skap2 is involved in integrin activation in B cells and macrophages (Togni et al., 2005; Alenghat et al., 2012). However, these previous studies failed to demonstrate the in vivo roles for Skap2 in integrin activation and neutrophil recruitment.

The SH3 domain of Skap2 is described to be crucial for binding of interaction partners. Skap2 interacts with ADAP via its SH3 domain (Marie-Cardine et al., 1998). In contrast to Skap2, ADAP is only involved in selectin- and not GPCR-mediated integrin activation (Block et al., 2012). This difference may be explained by the fact that ADAP and Skap2 act as scaffolding proteins for different signaling molecules. It is also conceivable that two independent modules of Skap2 exist in neutrophils, one interacting with ADAP and one with WASp, similar to how it was reported for Skap2/ADAP modules in T cells (Kliche et al., 2012). Here, we revealed for the first time that Skap2 interacts with WASp in primary neutrophils through W336K located in the Skap2 SH3 domain and that this residue is critical for Skap2 function and WASp translocation. However, we cannot completely rule out that the mutation only affects the binding of WASp because other interaction partners might also bind to this region in the SH3 domain.

Phosphorylation is an important process of regulating the activity of proteins of the WASp family. Tyrosine phosphorylation of WASp leads to an increased activation of the Arp2/3 complex without apparent need for other known activators like Cdc42 or PIP_2 (Cory et al., 2003). However, we found that the localization of WASp, but not its phosphorylation state, is altered in *Skap2*$^{-/-}$ neutrophils after activation, suggesting that phosphorylation alone is not a critical mediator of WASp activity during neutrophil activation. Our data are in line with a previous study showing that *Was*$^{-/-}$ neutrophils are unable to cluster β_2 integrins in vitro (Zhang et al., 2006). The data provided here confirm and extend the previous findings by demonstrating that WASp is involved in the regulation of integrin affinity and valency after stimulating neutrophils with chemokines or selectins through its ability to initiate actin polymerization.

Although *Skap2*$^{-/-}$ mice did not suffer from visible abnormalities, they exhibit significant leukocytosis, especially in their neutrophil populations. Leukocytosis occurs when leukocyte integrins are dysfunctional, leading to LAD and reduced leukocyte extravasation. LAD syndromes have been described in mice and humans and can be caused by loss-of-function mutations of β_2 integrins (Schmidt et al., 2013). Talins and kindlins, two families of FERM (4.1, ezrin, radixin, moesin)-domain proteins, bind the cytoplasmic tail of integrins, recruit cytoskeletal and signaling proteins involved in mechanotransduction, and synergize to activate integrin binding to extracellular ligands (Moser et al., 2009b; Shattil et al., 2010). Recruitment of both talin-1 and kindlin-3 to distinct binding sites of integrin cytoplasmic tails is critical for β_1, β_2, and β_3 integrin activation (Shattil et al., 2010). However, both molecules have distinct roles in integrin activity regulation and cooperate to facilitate neutrophil recruitment (Moser et al., 2009a; Lefort et al., 2012; Calderwood et al., 2013). The molecular mechanisms by which talin-1 and kindlin-3 bind integrin cytoplasmic tails and trigger integrin activation are well accepted, but how the recruitment of these molecules is regulated remains poorly understood (Calderwood et al., 2013). A Rap1/RIAM complex–dependent pathway targets talin-1 to the integrin β cytoplasmic tail, thereby mediating integrin activation (Lee et al., 2009; Klapproth et al., 2015). The small GTPase Rap1 has emerged as a key regulator in regulation of affinity and valency regulation of β_1, β_2, and β_3 integrins (Bos, 2005). Interestingly, in addition to the Rap1/RIAM-mediated signaling pathway, a Rap1-independent association of talin with integrins and subsequent integrin activation have been reported (Lee et al., 2013). It will be of interest to determine whether the Rap1-dependent talin-1 recruitment and the Skap2/WASp-dependent talin-1 and kindlin-3 recruitment to the integrin tail are two distinct processes or whether both act coordinately to induce integrin activation.

In addition to mediating integrin activation, integrin outside-in signaling is abolished in the absence of Skap2, suggesting that Skap2 is indispensable for both inside-out and outside-in signaling. Interestingly, Skap2 deficiency did not affect integrin activation in platelets (unpublished data), and we found no increased bleeding tendency in *Skap2*$^{-/-}$ mice after hepatic injury or renal ischemia reperfusion. Recent research revealed that $\alpha_{IIb}\beta_3$ integrin activation and function is dependent on the interaction of ADAP with talin-1 and

membrane localization. 75 cells/experiment were analyzed. *n* = 3. (F) Phosflow analysis of pAKT in *Skap2*$^{-/-}$ neutrophils reconstituted with the vector control, Skap2, or Skap2 R140M after stimulation with CXCL1. Fold-increase in pAKT compared with the unstimulated control is shown. *n* = 2. (G–I) IVM of TNF-inflamed postcapillary venules of WT mice after bone marrow transplantation of *Skap2*$^{-/-}$ hematopoietic stem cells retrovirally transduced with the vector control, Skap2, or Skap2ΔSH3. Rolling velocity (G), number of adherent cells (H), and number of extravasated cells (I) 2 h after TNF application are shown. *n* = 3 mice/group. (J) Soluble ICAM-1 binding of CXCL1-stimulated transduced *Skap2*$^{-/-}$ neutrophils. *n* = 3. (K) Expression of Skap2 in WT, *Skap2*$^{-/-}$, and *Skap2*$^{-/-}$ neutrophils reconstituted with Skap2, vector control, or Skap2 W336K. Lysates were immunoblotted with anti-Skap2 and anti-α-tubulin antibody. *n* = 2. The same experiment as in C is shown. (L–N) IVM of TNF-inflamed postcapillary venules of WT mice after bone marrow transplantation of *Skap2*$^{-/-}$ hematopoietic stem cells retrovirally transduced with the vector control, Skap2, or Skap2 W336K. Rolling velocity (L), number of adherent cells (M), and number of extravasated cells (N) 2 h after TNF application are shown. *n* = 3 mice/group. (O) Soluble ICAM-1 binding of CXCL1-stimulated reconstituted *Skap2*$^{-/-}$ neutrophils. *n* = 3. *, P < 0.05; **, P < 0.01; Student's *t* test (B), one-way ANOVA (E–I and L–N), or two-way ANOVA (J and O). Data are means ± SEM. Ctrl, control; MSCV, murine stem cell virus.

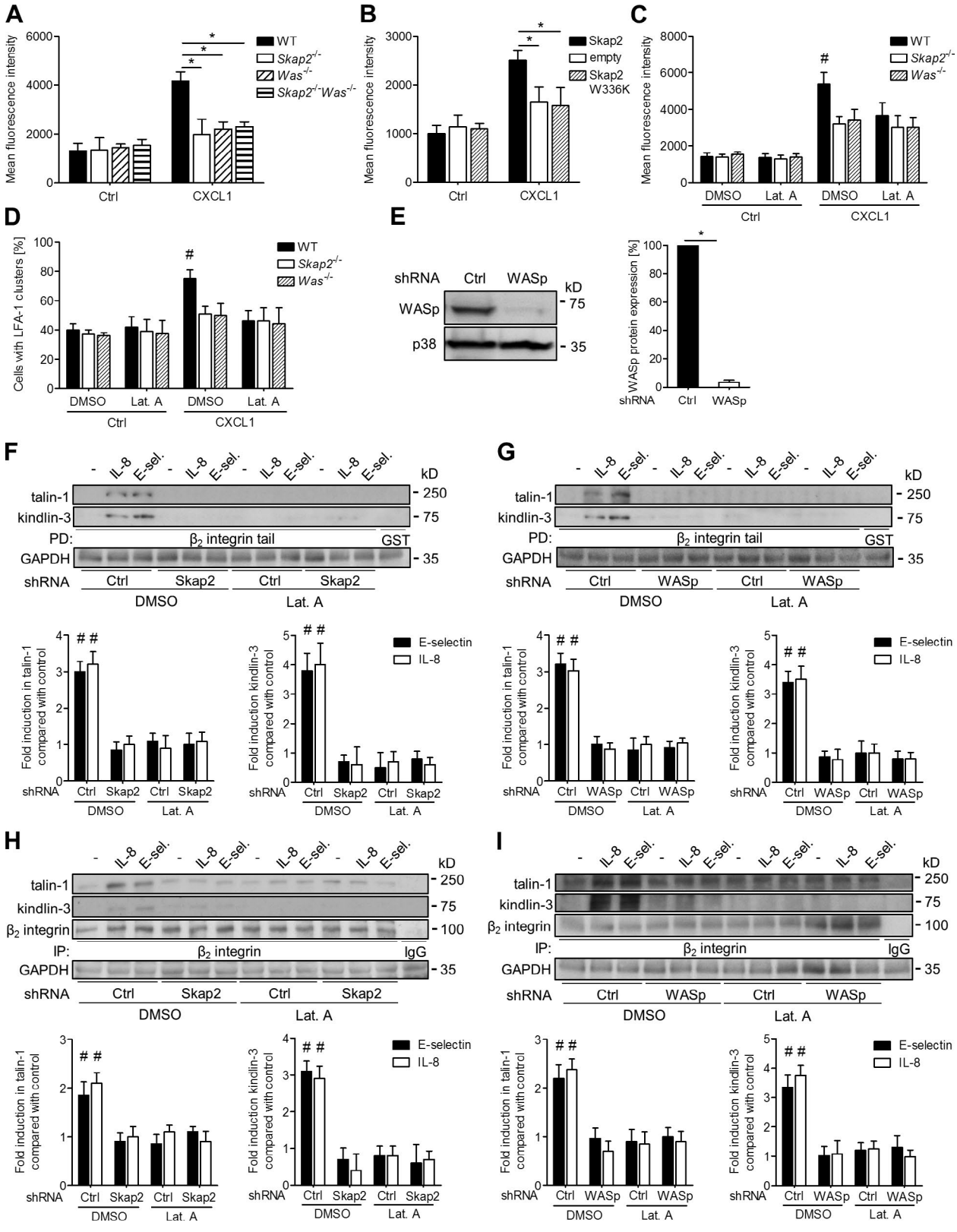

Figure 7. **The Skap2/WASp complex triggers actin polymerization, thereby enabling β_2 integrin activation by recruitment of talin-1 and kindlin-3.** (A and B) F-actin polymerization of WT, *Skap2*$^{-/-}$, *Was*$^{-/-}$, and *Skap2*$^{-/-}$*Was*$^{-/-}$ neutrophils (A) and *Skap2*$^{-/-}$ neutrophils reconstituted with vector control, Skap2, or Skap2 W336K (B) after stimulation with CXCL1 in solution. $n = 3$. (C and D) Soluble ICAM-1 binding (C) and LFA-clustering (D) of

kindlin-3. However, this interaction is independent of Skap2 (Kasirer-Friede et al., 2014). This is in agreement with our results and raises the important conclusion that Skap2 operates as an integrin-activating module both in a cell type– and integrin-specific manner.

Leukocyte recruitment into inflamed tissue is a hallmark of inflammation (Phillipson and Kubes, 2011; Herter and Zarbock, 2013). Previous studies clearly demonstrated that leukocytes recruited into inflamed tissue contribute to tissue damage and impair organ function. The blockage of the main signaling pathways involved in leukocyte recruitment had beneficial and protective effects (McDonald et al., 2010; Phillipson and Kubes, 2011; McDonald and Kubes, 2012; Volmering et al., 2016). This study shows for the first time the crucial and indispensable role of the special and unique cytosolic adaptor protein Skap2 in several different signaling pathways required for neutrophil recruitment, integrin activation, and neutrophil functions. The reduced neutrophil recruitment into the inflamed tissue and improved organ function in *Skap2*$^{-/-}$ mice show that the therapeutic blockade of this adaptor protein may be beneficial in sterile tissue injury or other inflammatory disorders.

MATERIAL AND METHODS

Animals

The 8–15-wk-old C57BL/6 (Janvier), *Skap2*$^{-/-}$ (Togni et al., 2005), *Was*$^{-/-}$ (Snapper et al., 1998), and *Skap2*$^{-/-}$*Was*$^{-/-}$ mice and littermate controls were housed in a specified pathogen–free facility. *Skap2*$^{-/-}$, *Was*$^{-/-}$, and *Skap2*$^{-/-}$*Was*$^{-/-}$ mice were backcrossed to a C57BL/6 background for at least nine generations. The Animal Care and Use Committees of the University of Münster approved all animal experiments.

Spinning disk confocal IVM of the mouse liver after focal hepatic necrosis

For IVM of the liver, mice were prepared as previously described (Volmering et al., 2016). In brief, mice were anesthetized and placed on a heating pad to maintain body temperature. To induce focal injury, a thin platinic wire was heated and shortly pressed on the exposed liver lobe. The liver lobe was exposed, but no focal injury was induced in sham-operated mice. The necrotic tissue was visualized by 40 ng/ml propidium iodide (Sigma-Aldrich), and neutrophils were labeled by i.v. injection of neutrophil-specific Alexa Fluor 488–conjugated Ly-6G antibody (clone 1A8; BioLegend). Immediately after preparation, the exposed liver was visualized with an upright spinning disk confocal microscope (CellObserver SD; ZEISS) equipped with a 5×/0.25 FLUAR objective, and time-lapse Z stacks were recorded for 4 h. The number of adherent neutrophils was determined for different time points per field of view by using FIJI. The serum levels of the transaminases GOT and GPT before and 4 h after focal hepatic necrosis of WT and *Skap2*$^{-/-}$ mice were determined with a hematology analyzer (ADVIA; Siemens).

IRI of the kidney

IRI was performed as described previously (Herter et al., 2013). In brief, mice were anesthetized and placed on a heating pad to maintain body temperature. For renal ischemia reperfusion, both renal pedicles were exposed and cross-clamped for 32 min with hemostatic microclips. After 32 min, the clamps were removed. Kidney pedicles were exposed but not clamped in sham-operated mice. Mice were euthanized, and blood samples were taken by heart puncture 24 h after surgery. Neutrophil recruitment into the kidneys was determined by flow cytometry as previously described (Herter et al., 2013). Serum creatinine levels were determined with a creatinine assay (Diazyme) according to the manufacturer's instructions. Neutrophil blood counts were determined by counting leukocytes using Kimura stain and analyzing the fraction of CD45^{hi} Ly6B.2^{hi} Gr-1^{hi} neutrophils in the blood after red blood cell depletion by flow cytometry.

Histological examination

Kidneys were fixated in 4% formaldehyde, embedded in paraffin, and sectioned at 2 µm for hematoxylin and eosin staining. Histopathological examinations were performed by two renal pathologists blinded to the conditions. Changes in the outer medulla, expressed as the acute tubular necrosis score, were scored by counting the percentage of tubules that displayed cell necrosis with loss of brush border and dilatation of tubules and/or cast formation as follows: 0, none; 1, <10%; 2, 11–25%; 3, 26–45%; 4, 46–75%; and 5, >76% (Li et al., 2010). For each slide, at least 7–10 fields were reviewed at a magnification of 200 (DM5500B; Leica Biosystems), and representative micrographs were made using the Diskus software package (Hilgers).

IVM of the mouse cremaster muscle

Inflammation was induced by intrascrotal injection of 500 ng recombinant mouse TNF-α (rmTNF-α; R&D Systems). The cremaster muscle was prepared for intravital imaging 2 h after

CXCL1-stimulated WT, *Skap2*$^{-/-}$, and *Was*$^{-/-}$ neutrophils after pretreatment with DMSO or Lat. A. For clustering, 50 cells/experiment were analyzed. $n = 3$. (E) Knockdown of WASp in HL-60 cells. Quantification is shown on the right. $n = 3$. (F–I) Control, Skap2, or WASp knockdown HL60 cells were pretreated with DMSO or Lat. A and left unstimulated, plated on E-selectin with shear, or stimulated with IL-8 in solution. Lysates were incubated with GST fusion proteins of the β_2 integrin cytoplasmic domain (F and G) or immunoprecipitated with anti-β_2 integrin antibody (H and I). Precipitates were immunoblotted with anti–talin-1 and anti–kindlin-3 or anti-β_2 integrin antibody, respectively. Input was immunoblotted with anti-GAPDH antibody. Quantifications are shown below. $n = 3$. *, $P < 0.001$; #, $P < 0.05$ versus all other groups; one-way ANOVA (A–B and F–I), two-way ANOVA (C and D), or Student's *t* test (E). Data are means ± SEM. Ctrl, control; E-Sel., E-selectin; IP, immunoprecipitate; PD, precipitate.

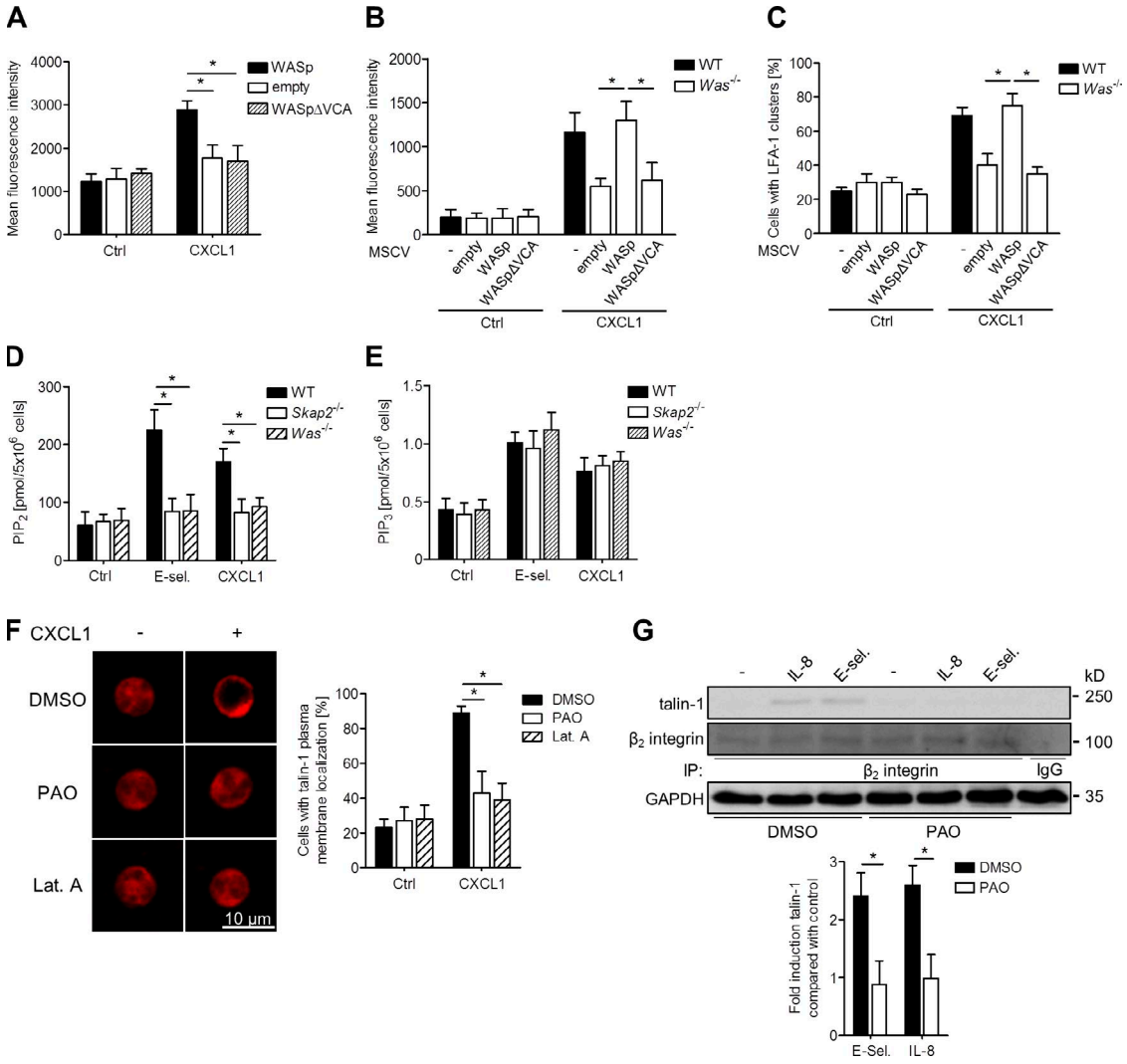

Figure 8. **Integrin activation is dependent on WASp-mediated de novo actin polymerization but also on PIP_2 synthesis.** (A–C) F-actin polymerization (A), soluble ICAM-1 binding (B), and LFA-1 clustering (C) of *Was*$^{-/-}$ neutrophils reconstituted with WASp, vector control, or a WASp mutant lacking the VCA domain (WASpΔVCA) after stimulation with CXCL1 in solution. $n = 3$. (D and E) PIP_2 (D) and PIP_3 (E) levels of WT, *Skap2*$^{-/-}$, and *Was*$^{-/-}$ neutrophils after CXCL1 stimulation in solution or plating on E-selectin with shear. $n = 2$. (F) Subcellular localization of talin-1 in unstimulated or CXCL1-stimulated WT neutrophils pretreated with DMSO, PAO, or Lat. A. Representative images and statistics of talin-1 plasma membrane localization are shown. 40 cells/experiment were analyzed. $n = 3$. (G) Immunoprecipitation of β_2 integrin in IL-8– or E-selectin–stimulated HL-60 cells after pretreatment with DMSO or PAO. Precipitates were immunoblotted with anti–talin-1 and anti–kindlin-3 or anti–β_2 integrin antibody. Input was immunoblotted with anti-GAPDH antibody. Quantification is shown below. $n = 3$. *, $P < 0.05$; one-way ANOVA (A and D–F), two-way ANOVA (B and C), or Student's *t* test (G). Data are means ± SEM. Ctrl, control; E-sel., E-selectin; IP, immunoprecipitate; MSCV, murine stem cell virus.

application. IVM was performed on an upright microscope (AxioSkop; ZEISS) with a 40 × 0.75 NA saline immersion objective. In some experiments, IVM was performed before and after superfusion of the cremaster muscle with 5 nM rmCXCL2 (R&D Systems) for 1 h at 20 ml/h. In vivo neutrophil rolling velocity and adhesion were determined by transillumination IVM of postcapillary venules with a diameter between 20 and 40 µm, whereas neutrophil extravasation was investigated by near-infrared reflected-light oblique transillumination microscopy, as described previously (Mueller et al., 2010). For E-selectin–mediated slow neutrophil rolling, 4 µg pertussis toxin (i.v.; Merck) was injected together with rmTNF-α 2 h before the experiment and a blocking P-selectin antibody (RB40.34) immediately before IVM. Analysis of recorded images was performed using AxioVision software (ZEISS). Emigrated cells were determined in an area of 75 × 100 µm to each side of a vessel (1.5×10^4 µm^2 tissue area). The microcirculation was recorded using a digital camera (Sensicam QE; PCO-Tech). For GPCR-mediated arrest, the initial number of adherent cells in a representative vessel was deter-

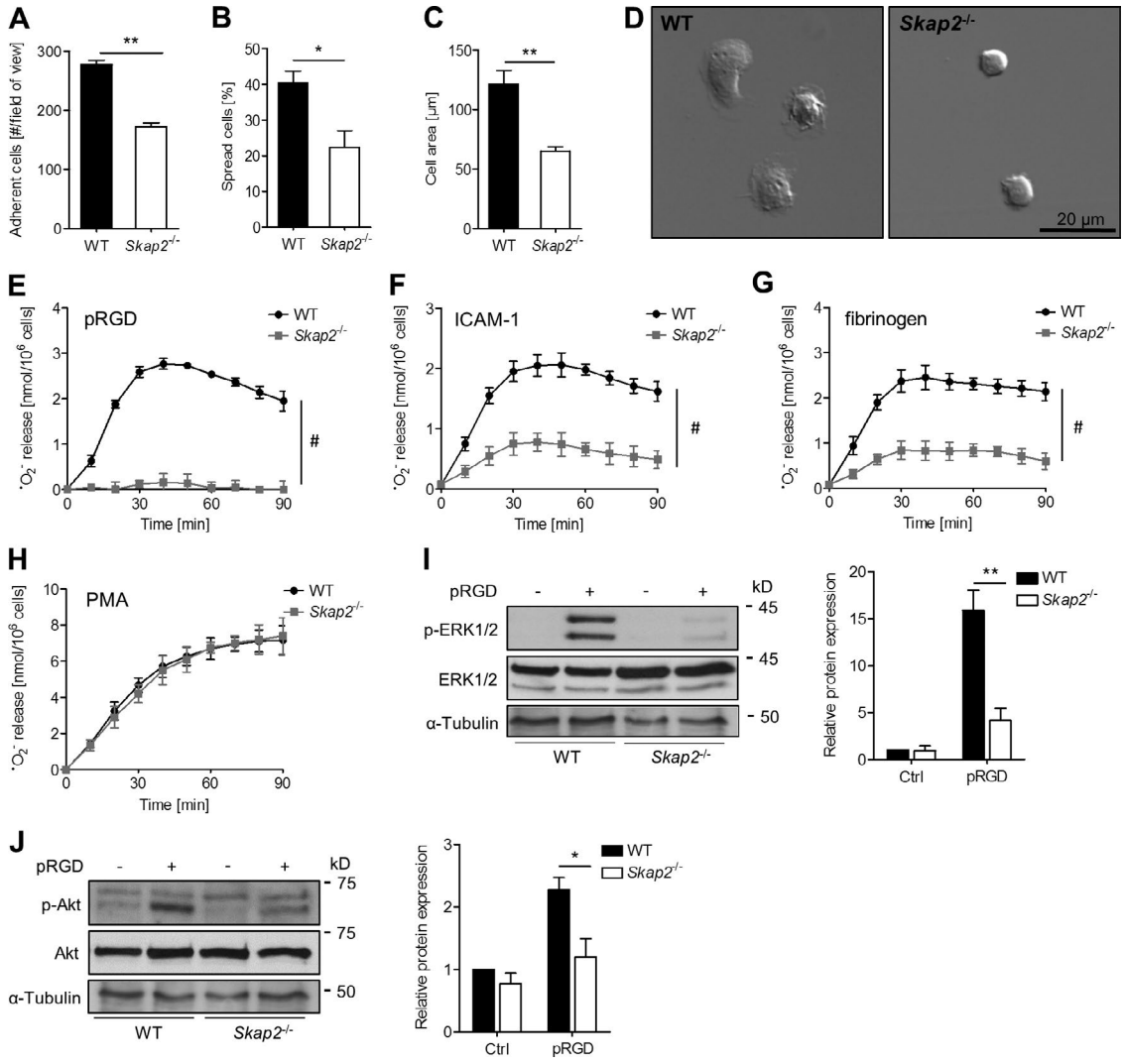

Figure 9. **Skap2 regulates integrin-mediated outside-in signaling.** (A–D) Neutrophils from WT or *Skap2*$^{-/-}$ mice were plated on pRGD and adhesion (A) and spreading (B and C) were analyzed. (D) Representative images of spread neutrophils. 75 cells/experiment were analyzed. $n = 3$. (E–G) Adhesion-dependent oxidative burst of WT and *Skap2*$^{-/-}$ neutrophils plated on pRGD alone (E) or ICAM-1 (F) and fibrinogen (G) in the presence of TNF. $n = 4$. (H) Oxidative burst of WT and *Skap2*$^{-/-}$ neutrophils stimulated with PMA in solution. $n = 4$. (I and J) WT and *Skap2*$^{-/-}$ neutrophils were plated on pRGD for 10 min, and lysates were immunoblotted with anti–p-ERK1/2 and anti-ERK1/2 (I) or anti–p-Akt and anti-Akt (J) and anti–α-tubulin antibody. Quantification is shown on the right. $n = 4$. *, $P < 0.05$; **, $P < 0.01$; #, $P < 0.05$ versus all other time points; Student's *t* test. Data are means ± SEM. Ctrl, control.

mined. After injection of 500 ng rmCXCL1 (R&D Systems) or 4 µg LTB_4 (Cayman Chemical) via the carotid artery, the vessel was recorded for 15 min. To perform adoptive transfer, bone marrow from WT and *Skap2*$^{-/-}$ mice was isolated and labeled with 2 µM green (CMFDA) or orange (CMRA) cell tracker (Invitrogen) according to the manufacturer's instructions. Cells were injected i.v. in a ratio of 1:1 into WT mice 30 min after intrascrotal injection of rmTNF-α. The rolling velocity was analyzed 2 h after TNF application. Adhesion and extravasation were determined as the percentage of total fluorescent cells. IVM of *Skap2*$^{-/-}$ mice after retroviral reconstitution of bone marrow cells was performed by epifluorescence microscopy with an AxioScopeA1 microscope (ZEISS) and a charged-coupled device camera (Sensicam QE). Epifluorescence was generated using a Lambda DG-4 system (Sutter Instrument). For intravascular crawling, mice were injected with neutrophil-specific Alexa Fluor 488–conjugated Ly-6G antibody before the experiment. The cremaster muscle was exteriorized and superfused with 5 nM MIP-2, and time-lapse microscopy was performed for 2 h. Adherent cells were quantified, and cell movement was analyzed using SlideBook software (Intelligent Imaging Innovations).

Peripheral blood cell counts

Whole blood was taken from the facial vein and collected in heparin-coated tubes. Blood cell counts were deter-

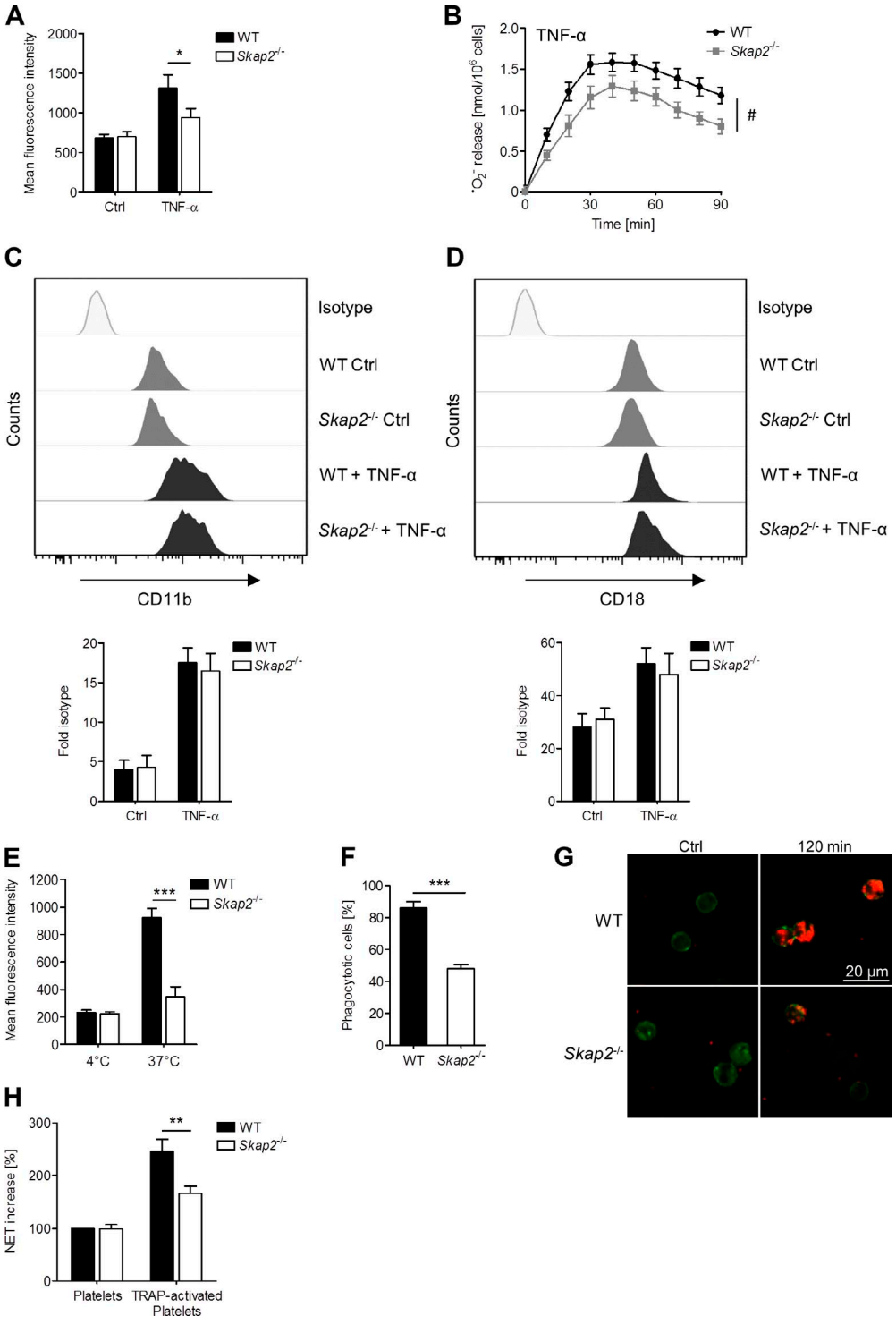

Figure 10. **Skap2 regulates TNF-mediated integrin activation and outside-in signaling as well as neutrophil functions.** (A) Soluble ICAM-1 binding of TNF-stimulated WT and *Skap2*$^{-/-}$ neutrophils. $n = 3$. (B) Oxidative burst of WT and *Skap2*$^{-/-}$ neutrophils stimulated with TNF in solution. $n = 3$. (C and D) Surface expression of CD11b (C) and CD18 (D) of TNF-stimulated WT or *Skap2*$^{-/-}$ neutrophils. Quantification is shown below. $n = 3$. (E–G) Phagocytosis of pHrodo *E. coli* particles by WT and *Skap2*$^{-/-}$ neutrophils. Phagocytosis (E), percentage of phagocytic cells (F), and representative images (G) of phagocytic neutrophils are shown. $n = 3$. (H) In vitro NET formation of WT and *Skap2*$^{-/-}$ neutrophils stimulated with resting or TRAP-activated platelets. $n = 3$. *, $P < 0.05$; **, $P < 0.01$; ***, $P < 0.001$; #, $P < 0.05$ versus all other time points; Student's *t* test. Data are means ± SEM. Ctrl, control.

mined using a hematology analyzer (scil Vet abc Plus+; scil animal care company).

Gene knockdown

HEK293T cells were transiently cotransfected with lentiviral packaging plasmids pVSV-G, pMDLg, p-RSV-Rev, and pLKO.1 vectors (Sigma-Aldrich) containing a specific shRNA sequence directed against human Skap2 (5′-CCG GGCAGATGTTGAAACATTTGTA CTCGAGTACAAA TGTTTCAACATCTGCTTTTT-3′), human WASp (5′-CCGGCGAGACCT CTAAACTTATCTACTCGAGTA GATAAGTTTAGAGGTCTCGTTTTT-3′), or control (5′-CCGGCAACAAGATGAAGAGCACCAACTCGAGTT GGTGCTCTTCATCTTGTTGTTTTTG-3′). Infection of promyelocytic HL60 cells was performed by incubation with medium containing lentiviral particles for 48 h. Stable knockdown of Skap2 and WASp in transduced HL60 cells was confirmed by Western blotting and maintained by puromycin selection (1 μg/ml; Sigma-Aldrich).

Autoperfused flow chamber systems

To investigate rolling velocity in vitro, rectangular glass capillaries (20 × 200 μm) were coated with 2.5 μg/ml rmE-selectin alone or in combination with 2 μg/ml rmICAM-1 for 2 h and then blocked for 2 h with 1% casein (Thermo Fisher Scientific). The capillary was connected to polyethylene tubing (BD) which was surgically inserted into the mouse carotid artery. 5–10 representative fields of view were recorded for 1 min with an immersion objective (SW40/0.75) and a digital camera (Sensicam QE). Rolled distance was analyzed with ImageJ (National Institutes of Health), and the rolling velocity was calculated. For chemokine-induced adhesion in vitro, glass capillaries were coated with 50 μg/ml rmP-selectin, 15 μg/ml rmICAM-1, and 25 μg/ml rmCXCL1 or 7.5 ng/ml PMA for 2 h and then blocked for 1 h with 1% casein. 5–10 representative fields of view were recorded after an initial perfusion period of 6 min, and the number of adherent cells was determined.

Soluble ICAM-1 and fibrinogen binding

Isolated bone marrow neutrophils or HL60 cells were suspended in ice-cold HBSS (Gibco), supplemented with 1.2 mM $CaCl_2$, 1 mM $MgCl_2$, and 10 mM Hepes, pH 7.4, and incubated with 10 μg/ml blocking anti–Mac-1 antibody (clone M1/70) for 10 min on ice. Then, neutrophils were stimulated with 100 ng/ml rmCXCL1 for 3 min, 150 nM PMA for 5 min or 3 mM Mn^{2+} for 3 min at 37°C, or left unstimulated in presence of 20 μg/ml ICAM-1/Fc and Fc-specific APC-conjugated anti–human IgG1 (SouthernBiotech). HL60 cells were stimulated with 100 ng/ml IL-8. Cells were fixated with 3.7% formaldehyde (Roth) for 10 min on ice, and neutrophils were stained with FITC-conjugated anti–Ly-6B.2 (clone 7/4; AbD Serotec) and analyzed by flow cytometry (5,000–10,000 cells per experiment). In some experiments, cells were incubated with 1 μM Lat. A (Sigma-Aldrich) or DMSO (Sigma-Aldrich) for 30 min at 37°C before stimulation.

For fibrinogen binding, neutrophils were stimulated with 100 ng/ml rmCXCL1 for 10 min at 37°C or left unstimulated in the presence of 150 μg/ml Alexa Fluor 647–conjugated fibrinogen (Invitrogen). HL60 cells were stimulated with 100 ng/ml IL-8. Negative controls were treated with 2 mM EDTA. Fluorescence intensity was analyzed by flow cytometry (5,000–10,000 cells per experiment). The percentage of neutrophils positive for fibrinogen binding was calculated by defining a threshold of the fluorescence intensity where 95% of neutrophils in the EDTA-treated control were considered as negative.

Reporter antibody flow chambers

Rectangular glass capillaries were precoated with 500 μg/ml protein G for 2 h. Capillaries were washed with PBS and coated with 6.6 μg/ml recombinant human E-selectin (rhE-selectin; R&D Systems) and 25 μg/ml mouse IgG1 (Santa Cruz Biotechnology, Inc.), 25 μg/ml activation-specific anti–β_2 integrin (clone KIM127; ATCC), or 10 μg/ml anti–LFA-1 (clone TS2/4; BioLegend) for 1 h and subsequently blocked with 1% casein. In another set of experiments, capillaries were coated with 20 μg/ml rhP-selectin (R&D Systems), 50 μg/ml rhIL-8 (PeproTech), and 5 μg/ml mouse IgG1, 5 μg/ml activation-specific anti-β_2 integrin (clone mAb24; provided by N. Hogg, Cancer Research UK London Research Institute, London, England, UK), 10 μg/ml anti–LFA-1 (clone TS2/4), 40 μg/ml activation-specific anti–Mac-1 (clone CBRM1/5; BioLegend), or 30 μg/ml anti–Mac-1 (clone M1/70; BioLegend). HL60 cells were resuspended in freshly isolated human plasma. The flow chamber was perfused with the cell suspension for 2 min and subsequently flushed with PBS containing 1 mM $MgCl_2$ and $CaCl_2$ for 1 min to remove nonadherent cells. 10 representative fields of view were recorded, and the number of adherent cells was determined.

Immunofluorescence and in vitro clustering

Isolated bone marrow neutrophils were suspended in PBS containing 1 mM $MgCl_2$ and $CaCl_2$. Cells were either stimulated on μ-Slide 8 wells (Ibidi) precoated with 10 μg/ml rmE-selectin for 10 min with shear or in solution by adding 100 ng/ml rmCXCL1 for 1 min at 37°C. Then, cells were fixated with 2% paraformaldehyde at room temperature and blocked with 3% BSA in PBS. After a 2-h incubation with Alexa Fluor 488–conjugated anti-Gr1 antibody (clone RB6-8C5) for plasma membrane staining, cells were permeabilized with 0.1% saponin and blocked with 3% BSA in PBS. Incubation with anti-WASp (clone H-250; Santa Cruz Biotechnology, Inc.), Alexa Fluor 405–conjugated anti-WASp (clone B-9; Santa Cruz Biotechnology, Inc.), anti-Skap2 (Proteintech), or anti–talin-1 (clone 8d4) with corresponding isotype control antibodies was performed at 4°C overnight. After incubation with Alexa Fluor 568– and 647–conjugated

secondary antibodies (Molecular Probes) for 1 h, cells were analyzed by confocal microscopy. In some experiments, cells were incubated with 2 µM PAO or DMSO for 15 min at 37°C before stimulation. For clustering, cells were incubated with Alexa Fluor 488– or 568–conjugated anti–LFA-1 (clone M17/4; BioLegend) at 4°C overnight. In some experiments, cells were incubated with 1 µM Lat. A or DMSO for 30 min at 37°C before stimulation. To analyze clustering, the mean fluorescence intensity of unstimulated cells was used as a cutoff to distinguish between clustered and not clustered cells. The Pearson's correlation coefficient (Pearson's R) was analyzed using ImageJ.

Constructs

Skap2 and WASp cDNA was obtained by reverse transcription PCR strategy from mouse neutrophil RNA. The Skap2-CC domain (40–122 aa), -PH domain (301–666 aa), and -SH3 domain (886–1,077 aa) fragments, truncated Skap2 lacking the SH3 domain (Skap2ΔSH3; 1–885 aa), and truncated WASp lacking the VCA domain (WASpΔVCA; 1–1,226 aa) were generated by PCR-based techniques. Skap2 mutations R140M and W336K were generated by QuickChange site-directed mutagenesis (Agilent Technologies). For expression of fusion proteins, cDNA was subcloned into pGEX-4T-2 (GE Healthcare) or pET30a (EMD Millipore). The cytoplasmic domain of CD18 cloned into pGEX-4T-1 was provided by S. Kliche (University of Magdeburg, Magdeburg, Germany). To generate recombinant retrovirus, cDNAs were subcloned in pMSCV-IRES-GFP II (pMIG II).

Recombinant protein expression and purification

Glutathione S-transferase (GST)- and polyhistidine (His)-tagged proteins were expressed in Rosetta 2(DE3) cells (EMD Millipore) growing in presence of chloramphenicol, ampicillin, and kanamycin (Sigma-Aldrich). Expression was induced by addition of 0.1 mM IPTG (AppliChem) for 6 h at 25°C or 18°C overnight. For purification of GST-tagged proteins, bacteria were suspended in Tris-buffered saline buffer containing PMSF and protease inhibitors (Roche) and subsequently sonificated. The supernatant was incubated with glutathione sepharose 4B (GE Healthcare) on an orbital mixer for 1 h at 4°C. Sepharose was washed and stored at 4°C until used. His-tagged proteins were purified using a His-Pur Ni-NTA Purification kit (Thermo Fisher Scientific) according to the manufacturer's instruction. Expression, purity, and concentration were determined by SDS-PAGE using Coomassie Brilliant blue staining.

Surface expression

Blood samples of WT and *Skap2*$^{-/-}$ mice were taken by heart puncture and depleted of red cells by hypotonic lysis. Cells were incubated with FITC-conjugated anti-Ly6B.2 and APC-conjugated anti-CD45 (clone 30-F11; BD) or PerCP-conjugated anti–Gr-1 and one of the following PE-conjugated antibodies for 30 min on ice in the dark: anti-CD11a (clone M17/4), anti-CD11b (clone M1/80), anti-CD162 (clone 2PH1), anti-CD62L (clone MEL-14), anti-CD44 (clone IM7; all from BD), anti-CXCR2 (clone 242216; R&D Systems), or respective isotype controls (BD). To assess the expression of CD11b and CD18 after stimulation, samples were stimulated for 30 min with 50 ng/ml TNF or left unstimulated in the presence of anti-CD11b (clone M1/80) and anti-CD18 (clone M18/2; BioLegend) antibodies. After fixation, cells were incubated with PE-conjugated secondary antibodies and analyzed by flow cytometry (5,000–10,000 cells per experiment). Neutrophils were gated as CD45^{hi} Ly6B.2^{hi} or Gr-1^{hi} Ly6B.2^{hi} cells, respectively.

Calcium flux

2×10^6 neutrophils were resuspended in Hepes-buffered Tyrode solution and incubated with 1 µM Indo-1 (Molecular Probes) for 1 h at 37°C. Cells were washed and resuspended in Hepes-buffered Tyrode solution with 1.25 mM calcium. Measurements were performed at 37°C by using a FluoroMax-2 spectrofluorometer, visualizing calcium flux after stimulation with 100 ng/ml CXCL1.

In vitro crawling

Isolated bone marrow neutrophils were seeded on polystyrene cell culture dishes (Corning) precoated for 4 h with mouse blood serum. Cells were incubated for 15 min at 37°C and 5% CO_2 and left untreated or stimulated with 10 nM rmCXCL2 for 5 min. Then, cell culture dishes were mounted on a parallel plate flow chamber (GlycoTech) and connected to a pump, and initial shear stress (10 dyn/cm^2 for 2 min) was applied. Time-lapse microscopy was performed without flow (5 min), during flow (shear stress 2 dyn/cm^2; 5 min), and after flow (5 min). Neutrophil movement was analyzed for each time phase with Manual Tracking (ImageJ) and the Chemotaxis and Migration Tool (Ibidi).

In vitro transmigration

bEnd.5 cells were seeded on 6.5-mm–diameter transwell filters with 5-µm pore size (Corning) precoated with 0.2% gelatin (Sigma-Aldrich). Cells were cultured until confluency and then stimulated with 5 nM rmTNF-α for 16 h. 0.5×10^6 isolated bone marrow neutrophils were applied to the upper reservoir. The lower reservoir was filled with medium with or without 40 ng/ml rmCXCL1. Plates were incubated at 37°C and 10% CO_2 for 30 min. The number of neutrophils in the lower reservoir was quantified with a Casy Cell Counter (Innovatis).

In vitro chemotaxis

Isolated bone marrow neutrophils were suspended in RPMI and seeded on chemotaxis µ-slides (2D; Ibidi) precoated with 50 µg/ml fibronectin (Sigma-Aldrich). The chemokine gradient was generated through diffusion by applying a Patentblue-colored (100 ng/ml) rmCXCL1 solution (1 µg/ml) to one reservoir of the slide according to the manufacturer's in-

structions. For control samples, a Patentblue-colored HBSS solution was applied. Chemotaxis was recorded with a microscope platform (37°C and 5% CO_2; Axio Observer; ZEISS) by using time-lapse microscopy at six frames per minute for 30 min. Cells were tracked manually with Manual Tracking (ImageJ) and analyzed with the Chemotaxis and Migration tool (Ibidi). Forward migration index represents the directness toward the gradient.

GST fusion protein pull-down assay and biochemical experiments

For GST pull-down, bone marrow neutrophils were isolated and suspended in PBS with 1 mM $CaCl_2$ and $MgCl_2$. Cells were left unstimulated or stimulated with 100 ng/ml CXCL1 for 5 min at 37°C or were applied to uncoated or rmE-selectin–precoated culture dishes for 10 min with shear. Then, neutrophils were lysed in NP-40 lysis buffer with protease inhibitors. Clarified lysates were precleared with unconjugated and GST-conjugated glutathione sepharose for 1 h at 4°C and subsequently incubated with 20 µg of glutathione Sepharose–conjugated GST fusion proteins for 4 h at 4°C. Samples were washed and analyzed by SDS-PAGE. For another set of experiments, HL60 cells were left unstimulated, stimulated with 100 ng/ml IL-8, or applied to uncoated or rhE-selectin–precoated culture dishes for 10 min with shear. Cells were lysed, and precleared samples were incubated with 30 µg of glutathione Sepharose–conjugated GST fusion proteins overnight at 4°C. In some experiments, cells were incubated with 1 µM Lat. A or DMSO for 30 min at 37°C before stimulation. Precipitates were washed and analyzed by SDS-PAGE, followed by immunoblotting with anti–talin-1 (clone 8d4; Sigma-Aldrich) and anti–kindlin-3 (clone 181A; EMD Millipore) antibodies. For immunoprecipitation, neutrophils were lysed in radioimmunoprecipitation assay buffer. Clarified lysates were precleared and then incubated with Sepharose G beads and anti-WASp or anti-Skap2 antibody (Proteintech) for 6 h at 4°C. Beads were washed, and bound proteins were eluted. Cell lysates and immunoprecipitates were immunoblotted with anti-phosphotyrosine or biotinylated anti-phosphotyrosine (clone 4G10; EMD Millipore), anti-WASp, or anti-Skap2 antibody and HRP-linked conformation-specific mouse anti–rabbit IgG. HL60 cells were lysed in NP-40/CHAPS (3-[(3-cholamidopropyl) dimethylammonio]-1-propanesulfonate) lysis buffer and immunoprecipitated with anti–β_2 integrin antibody (clone CTB104; BioLegend). Cells were pretreated with DMSO or 2 µM PAO for 15 min before stimulation with 100 ng/ml IL-8 for 3 min in solution or plating on uncoated or E-selectin–coated dishes with shear for 10 min. To analyze the expression of the different Skap2 and WASp constructs, bone marrow was isolated, GFP^+ neutrophils were sorted by FACS, and cells were lysed in radioimmunoprecipitation assay buffer. Immunoblots were developed using an enhanced chemilumescent system (GE Healthcare). Quantifications were performed using ImageJ.

In vitro protein binding

50 nM recombinant glutathione Sepharose–conjugated GST, GST-CC, GST-PH, GST-SH3, GST-SH3-W336K, or GST-Skap2 were incubated with 100 nM recombinant His-WASp in binding buffer (50 mM Tris-HCl, pH 7.4, 20 mM NaCl, and 0.05% Triton X-100) with shaking for 30 min at room temperature. After washing, bound proteins were eluted with sample buffer and analyzed by SDS-PAGE, followed by immunoblot analysis with anti-His, anti-GST (both Cell Signaling Technology), or anti-WASp antibody.

Hematopoietic stem cell isolation and retroviral transduction

Isolation and transduction of hematopoietic stem cells was performed as previously described (Block et al., 2012). In brief, supernatants containing viral particles were generated by transfecting the retrovirus-packaging cell line plate-E using Nanofectin (PAA). Lineage-negative hematopoietic stem and progenitor cells from *Skap2*$^{-/-}$ or *Was*$^{-/-}$ bone marrow were purified using a lineage cell depletion kit (Miltenyi Biotec) according to the manufacturer's instruction and cultured overnight at 37°C and 5% CO_2. For transduction, cells were applied to retrovirus-concentrated dishes and incubated overnight for infection. 2 d later, transduction efficiency was measured by flow cytometry. 2×10^6 cells with a mean transduction efficiency of 15–61% were injected i.v. into lethally irradiated (9.5 Gy) WT mice. Experiments were performed 6 wk after bone marrow transplantation, and transduced neutrophils were identified as GFP^+ cells.

Phosflow analysis

Reconstituted neutrophils were isolated and left unstimulated or stimulated with 100 ng/ml rmCXCL1 for 3 min at 37°C. Cells were immediately fixed with 1.5% formaldehyde for 10 min at room temperature, permeabilized with prechilled ethanol for 10 min on ice, and stained with PE-conjugated anti–phospho-Akt (S473; BD) for 45 min on ice. After washing, cells were stained with APC-conjugated anti-Gr1 and analyzed by flow cytometry.

PIP_2/PIP_3 ELISA

Isolated bone marrow neutrophils were left unstimulated or stimulated with 100 ng/ml CXCL1 for 1 min at 37°C or were applied to rmE-selectin–precoated culture dishes for 10 min with shear. Phosphatidylinositol polyphosphates were isolated, and PIP_2 or PIP_3 levels were analyzed with an ELISA assay (Echelon) according to the manufacturer's instructions.

F-actin polymerization

Isolated bone marrow neutrophils were left unstimulated or stimulated with 100 ng/ml rmCXCL1 for 5 min at 37°C and fixated with 3.7% formaldehyde for 30 min. Cells were washed and incubated with 0.5% Triton X-100 and Alexa Fluor 488– or 647–labeled phalloidin (Molecular Probes) for 30 min at room temperature. In some experiments, cells were

incubated with 1 µM Lat. A or DMSO for 30 min at 37°C before stimulation. After washing, cells were stained with APC- or FITC-conjugated anti-Gr1 and analyzed by flow cytometry (5,000–10,000 cells per experiment).

Static adhesion and spreading

Isolated bone marrow neutrophils were applied to glass coverslips, precoated with 20 µg/ml pRGD (Sigma-Aldrich) in the presence of 1 mM $CaCl_2$ and $MgCl_2$, and incubated for 30 min at 37°C and 5% CO_2. Coverslips were washed with PBS, and cells were fixated with 2.5% glutaraldehyde for 2 h at 4°C. The number of adherent and spread cells was determined by acquisition of differential interference contrast images with an Axio Observer microscope platform (ZEISS) equipped with an EC Plan-Neofluar 40×/1.30 oil differential interference contrast objective (ZEISS). Spreading area was determined using ImageJ software.

Oxidative burst

Isolated bone marrow neutrophils were applied to pRGD (20 µg/ml)-, ICAM-1 (1 µg/ml)–, or fibrinogen (150 µg/ml)-precoated 96-well plates (Immunolon-4 HBX; Thermo Fisher Scientific) with 1 mM $CaCl_2$, 1 mM $MgCl_2$, 0.1 mM cytochrome c (Sigma-Aldrich), and 50 ng/ml rmTNF-α, where indicated. For oxidative burst in suspension, wells were blocked with 10% FCS for 1 h at 37°C, and cells were stimulated with 100 nM PMA (Sigma-Aldrich) or 1 µg/ml rmTNF-α. 45 units of superoxide dismutase (Sigma-Aldrich) were added to each control sample to confirm that reduction of cytochrome c was mediated by superoxide production. Absorbance at 550 and 490 nm was recorded every 10 min for 90 min at 37°C in a plate reader. For calculation, each wavelength value was corrected by its superoxide dismutase control value.

Phagocytosis

pHrodo-labeled *E. coli* bioparticles (Molecular Probes) were opsonized with 50% mouse serum at 37°C for 30 min. Isolated bone marrow neutrophils were incubated with opsonized bioparticles at 37°C and 5% CO_2 for 2 h at a ratio of 1:10 (neutrophils/bioparticles). Negative controls were kept 2 h on ice. Cells were washed, fixed, stained with FITC-conjugated anti–Ly-6B.2, and analyzed by flow cytometry (5,000–10,000 cells per experiment). The percentage of phagocytosis at 4°C was deduced from the phagocytosis percentage at 37°C.

In vitro NET formation

Isolated neutrophils were resuspended in RPMI 1640 medium (PAN Biotech) with 1% fetal calf serum. Citrate-anticoagulated whole blood was obtained from WT mice, and platelets were isolated by low-speed centrifugation. 10^5 neutrophils were incubated with 10^6 platelets pretreated with or without 50 µM TRAP for 60 min at 37°C. To measure the amount of NET structures in the supernatant, we performed an ELISA as described previously (Caudrillier et al., 2012).

Statistics

Results are expressed as means ± SEM. Differences between the groups were evaluated by Student's *t* test, one-way ANOVA with posthoc Bonferroni correction, or two-way ANOVA, where appropriate (GraphPad Software). A p-value of <0.05 was considered statistically significant.

Online supplemental material

Video 1 shows the recruitment of Alexa Fluor 488–Ly6G–labeled neutrophils to the site of focal hepatic necrosis in WT mice. Video 2 shows the recruitment of Alexa Fluor 488–Ly6G–labeled neutrophils to the site of focal hepatic necrosis in *Skap2*$^{-/-}$ mice. Video 3 shows crawling of Alexa Fluor 488–Ly6G–labeled neutrophils in response to CXCL2 in WT mice. Video 4 shows crawling of Alexa Fluor 488–Ly6G–labeled neutrophils in response to CXCL2 in *Skap2*$^{-/-}$ mice.

ACKNOWLEDGMENTS

The authors would like to thank Stefan Volkery and Charlotte Sohlbach for expert technical support.

This work was supported by the Deutsche Forschungsgemeinschaft (grant nos. ZA428/12-1 and SFB1009_A5 to A. Zarbock), IZKF Münster (IZKF Za2/001/14 to A. Zarbock), and the National Institutes of Health (grant nos. RO1 AI068150 and AI113272 to C. Lowell).

The authors declare no competing financial interests.

Author contributions: M. Boras performed experiments, analyzed the data, and wrote the manuscript. S. Volmering performed experiments and analyzed the data. A. Bokemeyer, J. Rossaint, H. Block, and B. Bardel performed experiments. V. Van Marck and B. Heitplatz performed histological examinations. S. Kliche provided knockout animals and contributed to writing the manuscript. A. Reinhold provided knockout animals. C. Lowell interpreted data and contributed to writing the manuscript. A. Zarbock designed the study, analyzed the results, and wrote the manuscript.

Submitted: 4 May 2016
Revised: 3 November 2016
Accepted: 27 December 2016

REFERENCES

Alenghat, F.J., Q.J. Baca, N.T. Rubin, L.I. Pao, T. Matozaki, C.A. Lowell, D.E. Golan, B.G. Neel, and K.D. Swanson. 2012. Macrophages require Skap2 and Sirpα for integrin-stimulated cytoskeletal rearrangement. *J. Cell Sci.* 125:5535–5545. http://dx.doi.org/10.1242/jcs.111260

Altieri, D.C., F.R. Agbanyo, J. Plescia, M.H. Ginsberg, T.S. Edgington, and E.F. Plow. 1990. A unique recognition site mediates the interaction of fibrinogen with the leukocyte integrin Mac-1 (CD11b/CD18). *J. Biol. Chem.* 265:12119–12122.

Asazuma, N., J.I. Wilde, O. Berlanga, M. Leduc, A. Leo, E. Schweighoffer, V. Tybulewicz, C. Bon, S.K. Liu, C.J. McGlade, et al. 2000. Interaction of linker for activation of T cells with multiple adapter proteins in platelets activated by the glycoprotein VI-selective ligand, convulxin. *J. Biol. Chem.* 275:33427–33434. http://dx.doi.org/10.1074/jbc.M001439200

Bergmeier, W., T. Goerge, H.-W. Wang, J.R. Crittenden, A.C.W. Baldwin, S.M. Cifuni, D.E. Housman, A.M. Graybiel, and D.D. Wagner. 2007. Mice lacking the signaling molecule CalDAG-GEFI represent a model for leukocyte adhesion deficiency type III. *J. Clin. Invest.* 117:1699–1707. http://dx.doi.org/10.1172/JCI30575

Berzat, A., and A. Hall. 2010. Cellular responses to extracellular guidance cues. *EMBO J.* 29:2734–2745. http://dx.doi.org/10.1038/emboj.2010.170

Block, H., J.M. Herter, J. Rossaint, A. Stadtmann, S. Kliche, C.A. Lowell, and A. Zarbock. 2012. Crucial role of SLP-76 and ADAP for neutrophil recruitment in mouse kidney ischemia-reperfusion injury. *J. Exp. Med.* 209:407–421. http://dx.doi.org/10.1084/jem.20111493

Bos, J.L. 2005. Linking Rap to cell adhesion. *Curr. Opin. Cell Biol.* 17:123–128. http://dx.doi.org/10.1016/j.ceb.2005.02.009

Calderwood, D.A., I.D. Campbell, and D.R. Critchley. 2013. Talins and kindlins: partners in integrin-mediated adhesion. *Nat. Rev. Mol. Cell Biol.* 14:503–517. http://dx.doi.org/10.1038/nrm3624

Carman, C.V., and T.A. Springer. 2003. Integrin avidity regulation: are changes in affinity and conformation underemphasized? *Curr. Opin. Cell Biol.* 15:547–556. http://dx.doi.org/10.1016/j.ceb.2003.08.003

Caudrillier, A., K. Kessenbrock, B.M. Gilliss, J.X. Nguyen, M.B. Marques, M. Monestier, P. Toy, Z. Werb, and M.R. Looney. 2012. Platelets induce neutrophil extracellular traps in transfusion-related acute lung injury. *J. Clin. Invest.* 122:2661–2671. http://dx.doi.org/10.1172/JCI61303

Cory, G.O.C., R. Cramer, L. Blanchoin, and A.J. Ridley. 2003. Phosphorylation of the WASP-VCA domain increases its affinity for the Arp2/3 complex and enhances actin polymerization by WASP. *Mol. Cell.* 11:1229–1239. http://dx.doi.org/10.1016/S1097-2765(03)00172-2

Friedewald, J.J., and H. Rabb. 2004. Inflammatory cells in ischemic acute renal failure. *Kidney Int.* 66:486–491. http://dx.doi.org/10.1111/j.1523-1755.2004.761_3.x

Goksoy, E., Y.-Q. Ma, X. Wang, X. Kong, D. Perera, E.F. Plow, and J. Qin. 2008. Structural basis for the autoinhibition of talin in regulating integrin activation. *Mol. Cell.* 31:124–133. http://dx.doi.org/10.1016/j.molcel.2008.06.011

Helgeson, L.A., J.G. Prendergast, A.R. Wagner, M. Rodnick-Smith, and B.J. Nolen. 2014. Interactions with actin monomers, actin filaments, and Arp2/3 complex define the roles of WASP family proteins and cortactin in coordinately regulating branched actin networks. *J. Biol. Chem.* 289:28856–28869. http://dx.doi.org/10.1074/jbc.M114.587527

Herter, J., and A. Zarbock. 2013. Integrin regulation during leukocyte recruitment. *J. Immunol.* 190:4451–4457. http://dx.doi.org/10.4049/jimmunol.1203179

Herter, J.M., J. Rossaint, H. Block, H. Welch, and A. Zarbock. 2013. Integrin activation by P-Rex1 is required for selectin-mediated slow leukocyte rolling and intravascular crawling. *Blood.* 121:2301–2310. http://dx.doi.org/10.1182/blood-2012-09-457085

Kasirer-Friede, A., J. Kang, B. Kahner, F. Ye, M.H. Ginsberg, and S.J. Shattil. 2014. ADAP interactions with talin and kindlin promote platelet integrin αIIbβ3 activation and stable fibrinogen binding. *Blood.* 123:3156–3165. http://dx.doi.org/10.1182/blood-2013-08-520627

Khvotchev, M., and T.C. Südhof. 1998. Newly synthesized phosphatidylinositol phosphates are required for synaptic norepinephrine but not glutamate or γ-aminobutyric acid (GABA) release. *J. Biol. Chem.* 273:21451–21454. http://dx.doi.org/10.1074/jbc.273.34.21451

Klapproth, S., M. Sperandio, E.M. Pinheiro, M. Prünster, O. Soehnlein, F.B. Gertler, R. Fässler, and M. Moser. 2015. Loss of the Rap1 effector RIAM results in leukocyte adhesion deficiency due to impaired β2 integrin function in mice. *Blood.* 126:2704–2712. http://dx.doi.org/10.1182/blood-2015-05-647453

Kliche, S., T. Worbs, X. Wang, J. Degen, I. Patzak, B. Meineke, M. Togni, M. Moser, A. Reinhold, F. Kiefer, et al. 2012. CCR7-mediated LFA-1 functions in T cells are regulated by 2 independent ADAP/SKAP55 modules. *Blood.* 119:777–785. http://dx.doi.org/10.1182/blood-2011-06-362269

Königsberger, S., D. Peckl-Schmid, N. Zaborsky, I. Patzak, F. Kiefer, and G. Achatz. 2010. HPK1 associates with SKAP-HOM to negatively regulate Rap1-mediated B-lymphocyte adhesion. *PLoS One.* 5:e12468 . http://dx.doi.org/10.1371/journal.pone.0012468

Kumar, S., J. Xu, C. Perkins, F. Guo, S. Snapper, F.D. Finkelman, Y. Zheng, and M.D. Filippi. 2012. Cdc42 regulates neutrophil migration via crosstalk between WASp, CD11b, and microtubules. *Blood.* 120:3563–3574. http://dx.doi.org/10.1182/blood-2012-04-426981

Kuwano, Y., O. Spelten, H. Zhang, K. Ley, and A. Zarbock. 2010. Rolling on E- or P-selectin induces the extended but not high-affinity conformation of LFA-1 in neutrophils. *Blood.* 116:617–624. http://dx.doi.org/10.1182/blood-2010-01-266122

Lee, H.S., C.J. Lim, W. Puzon-McLaughlin, S.J. Shattil, and M.H. Ginsberg. 2009. RIAM activates integrins by linking talin to ras GTPase membrane-targeting sequences. *J. Biol. Chem.* 284:5119–5127. http://dx.doi.org/10.1074/jbc.M807117200

Lee, H.S., P. Anekal, C.J. Lim, C.C. Liu, and M.H. Ginsberg. 2013. Two modes of integrin activation form a binary molecular switch in adhesion maturation. *Mol. Biol. Cell.* 24:1354–1362. http://dx.doi.org/10.1091/mbc.E12-09-0695

Lefort, C.T., and K. Ley. 2012. Neutrophil arrest by LFA-1 activation. *Front. Immunol.* 3:157. http://dx.doi.org/10.3389/fimmu.2012.00157

Lefort, C.T., J. Rossaint, M. Moser, B.G. Petrich, A. Zarbock, S.J. Monkley, D.R. Critchley, M.H. Ginsberg, R. Fässler, and K. Ley. 2012. Distinct roles for talin-1 and kindlin-3 in LFA-1 extension and affinity regulation. *Blood.* 119:4275–4282. http://dx.doi.org/10.1182/blood-2011-08-373118

Ley, K., D.C. Bullard, M.L. Arbonés, R. Bosse, D. Vestweber, T.F. Tedder, and A.L. Beaudet. 1995. Sequential contribution of L- and P-selectin to leukocyte rolling in vivo. *J. Exp. Med.* 181:669–675. http://dx.doi.org/10.1084/jem.181.2.669

Ley, K., C. Laudanna, M.I. Cybulsky, and S. Nourshargh. 2007. Getting to the site of inflammation: the leukocyte adhesion cascade updated. *Nat. Rev. Immunol.* 7:678–689. http://dx.doi.org/10.1038/nri2156

Li, L., L. Huang, S.S. Sung, P.I. Lobo, M.G. Brown, R.K. Gregg, V.H. Engelhard, and M.D. Okusa. 2007. NKT cell activation mediates neutrophil IFN-γ production and renal ischemia-reperfusion injury. *J. Immunol.* 178:5899–5911. http://dx.doi.org/10.4049/jimmunol.178.9.5899

Li, L., L. Huang, A.L. Vergis, H. Ye, A. Bajwa, V. Narayan, R.M. Strieter, D.L. Rosin, and M.D. Okusa. 2010. IL-17 produced by neutrophils regulates IFN-γ–mediated neutrophil migration in mouse kidney ischemia-reperfusion injury. *J. Clin. Invest.* 120:331–342. http://dx.doi.org/10.1172/JCI38702

Macias, M.J., S. Wiesner, and M. Sudol. 2002. WW and SH3 domains, two different scaffolds to recognize proline-rich ligands. *FEBS Lett.* 513:30–37. http://dx.doi.org/10.1016/S0014-5793(01)03290-2

Marie-Cardine, A., L.R. Hendricks-Taylor, N.J. Boerth, H. Zhao, B. Schraven, and G.A. Koretzky. 1998. Molecular interaction between the Fyn-associated protein SKAP55 and the SLP-76-associated phosphoprotein SLAP-130. *J. Biol. Chem.* 273:25789–25795. http://dx.doi.org/10.1074/jbc.273.40.25789

McDonald, B., and P. Kubes. 2012. Neutrophils and intravascular immunity in the liver during infection and sterile inflammation. *Toxicol. Pathol.* 40:157–165. http://dx.doi.org/10.1177/0192623311427570

McDonald, B., K. Pittman, G.B. Menezes, S.A. Hirota, I. Slaba, C.C.M. Waterhouse, P.L. Beck, D.A. Muruve, and P. Kubes. 2010. Intravascular danger signals guide neutrophils to sites of sterile inflammation. *Science.* 330:362–366. http://dx.doi.org/10.1126/science.1195491

McEver, R.P. 2015. Selectins: initiators of leucocyte adhesion and signalling at the vascular wall. *Cardiovasc. Res.* 107:331–339. http://dx.doi.org/10.1093/cvr/cvv154

Micheva, K.D., R.W. Holz, and S.J. Smith. 2001. Regulation of presynaptic phosphatidylinositol 4,5-biphosphate by neuronal activity. *J. Cell Biol.* 154:355–368. http://dx.doi.org/10.1083/jcb.200102098

Moser, M., M. Bauer, S. Schmid, R. Ruppert, S. Schmidt, M. Sixt, H.-V. Wang, M. Sperandio, and R. Fässler. 2009a. Kindlin-3 is required for β_2 integrin–mediated leukocyte adhesion to endothelial cells. *Nat. Med.* 15:300–305. http://dx.doi.org/10.1038/nm.1921

Moser, M., K.R. Legate, R. Zent, and R. Fässler. 2009b. The tail of integrins, talin, and kindlins. *Science.* 324:895–899. http://dx.doi.org/10.1126/science.1163865

Mueller, H., A. Stadtmann, H. Van Aken, E. Hirsch, D. Wang, K. Ley, and A. Zarbock. 2010. Tyrosine kinase Btk regulates E-selectin-mediated integrin activation and neutrophil recruitment by controlling phospholipase C (PLC) γ2 and PI3Kγ pathways. *Blood.* 115:3118–3127. http://dx.doi.org/10.1182/blood-2009-11-254185

Nathan, C. 2006. Neutrophils and immunity: challenges and opportunities. *Nat. Rev. Immunol.* 6:173–182. http://dx.doi.org/10.1038/nri1785

Phillipson, M., and P. Kubes. 2011. The neutrophil in vascular inflammation. *Nat. Med.* 17:1381–1390. http://dx.doi.org/10.1038/nm.2514

Phillipson, M., B. Heit, P. Colarusso, L. Liu, C.M. Ballantyne, and P. Kubes. 2006. Intraluminal crawling of neutrophils to emigration sites: a molecularly distinct process from adhesion in the recruitment cascade. *J. Exp. Med.* 203:2569–2575. http://dx.doi.org/10.1084/jem.20060925

Robinson, M.K., D. Andrew, H. Rosen, D. Brown, S. Ortlepp, P. Stephens, and E.C. Butcher. 1992. Antibody against the Leu-CAM beta-chain (CD18) promotes both LFA-1- and CR3-dependent adhesion events. *J. Immunol.* 148:1080–1085.

Schmidt, S., M. Moser, and M. Sperandio. 2013. The molecular basis of leukocyte recruitment and its deficiencies. *Mol. Immunol.* 55:49–58. http://dx.doi.org/10.1016/j.molimm.2012.11.006

Shattil, S.J., C. Kim, and M.H. Ginsberg. 2010. The final steps of integrin activation: the end game. *Nat. Rev. Mol. Cell Biol.* 11:288–300. http://dx.doi.org/10.1038/nrm2871

Smith, M.L., T.S. Olson, and K. Ley. 2004. CXCR2- and E-selectin–induced neutrophil arrest during inflammation in vivo. *J. Exp. Med.* 200:935–939. http://dx.doi.org/10.1084/jem.20040424

Snapper, S.B., F.S. Rosen, E. Mizoguchi, P. Cohen, W. Khan, C.H. Liu, T.L. Hagemann, S.P. Kwan, R. Ferrini, L. Davidson, et al. 1998. Wiskott-Aldrich syndrome protein-deficient mice reveal a role for WASP in T but not B cell activation. *Immunity.* 9:81–91. http://dx.doi.org/10.1016/S1074-7613(00)80590-7

Song, X., J. Yang, J. Hirbawi, S. Ye, H.D. Perera, E. Goksoy, P. Dwivedi, E.F. Plow, R. Zhang, and J. Qin. 2012. A novel membrane-dependent on/off switch mechanism of talin FERM domain at sites of cell adhesion. *Cell Res.* 22:1533–1545. http://dx.doi.org/10.1038/cr.2012.97

Stadtmann, A., L. Brinkhaus, H. Mueller, J. Rossaint, M. Bolomini-Vittori, W. Bergmeier, H. Van Aken, D.D. Wagner, C. Laudanna, K. Ley, and A. Zarbock. 2011. Rap1a activation by CalDAG-GEFI and p38 MAPK is involved in E-selectin-dependent slow leukocyte rolling. *Eur. J. Immunol.* 41:2074–2085. http://dx.doi.org/10.1002/eji.201041196

Swanson, K.D., Y. Tang, D.F. Ceccarelli, F. Poy, J.P. Sliwa, B.G. Neel, and M.J. Eck. 2008. The Skap-hom dimerization and PH domains comprise a 3′-phosphoinositide-gated molecular switch. *Mol. Cell.* 32:564–575. http://dx.doi.org/10.1016/j.molcel.2008.09.022

Tanaka, M., S. Shimamura, S. Kuriyama, D. Maeda, A. Goto, and N. Aiba. 2016. SKAP2 promotes podosome formation to facilitate tumor-associated macrophage infiltration and metastatic progression. *Cancer Res.* 76:358–369. http://dx.doi.org/10.1158/0008-5472.CAN-15-1879

Thrasher, A.J., and S.O. Burns. 2010. WASP: a key immunological multitasker. *Nat. Rev. Immunol.* 10:182–192. http://dx.doi.org/10.1038/nri2724

Togni, M., K.D. Swanson, S. Reimann, S. Kliche, A.C. Pearce, L. Simeoni, D. Reinhold, J. Wienands, B.G. Neel, B. Schraven, and A. Gerber. 2005. Regulation of in vitro and in vivo immune functions by the cytosolic adaptor protein SKAP-HOM. *Mol. Cell. Biol.* 25:8052–8063. http://dx.doi.org/10.1128/MCB.25.18.8052-8063.2005

van Rheenen, J., and K. Jalink. 2002. Agonist-induced PIP_2 hydrolysis inhibits cortical actin dynamics: regulation at a global but not at a micrometer scale. *Mol. Biol. Cell.* 13:3257–3267. http://dx.doi.org/10.1091/mbc.E02-04-0231

Várnai, P., and T. Balla. 1998. Visualization of phosphoinositides that bind pleckstrin homology domains: calcium- and agonist-induced dynamic changes and relationship to myo-[^{3}H]inositol-labeled phosphoinositide pools. *J. Cell Biol.* 143:501–510. http://dx.doi.org/10.1083/jcb.143.2.501

Volmering, S., H. Block, M. Boras, C.A. Lowell, and A. Zarbock. 2016. The neutrophil Btk signalosome regulates integrin activation during sterile inflammation. *Immunity.* 44:73–87. http://dx.doi.org/10.1016/j.immuni.2015.11.011

Wiedemann, C., T. Schäfer, and M.M. Burger. 1996. Chromaffin granule-associated phosphatidylinositol 4-kinase activity is required for stimulated secretion. *EMBO J.* 15:2094–2101.

Zarbock, A., C.A. Lowell, and K. Ley. 2007. Spleen tyrosine kinase Syk is necessary for E-selectin-induced a_Lb_2 integrin-mediated rolling on intercellular adhesion molecule-1. *Immunity.* 26:773–783. http://dx.doi.org/10.1016/j.immuni.2007.04.011

Zhang, H., U.Y. Schaff, C.E. Green, H. Chen, M.R. Sarantos, Y. Hu, D. Wara, S.I. Simon, and C.A. Lowell. 2006. Impaired integrin-dependent function in Wiskott-Aldrich syndrome protein-deficient murine and human neutrophils. *Immunity.* 25:285–295. http://dx.doi.org/10.1016/j.immuni.2006.06.014